AD-A072 421 SYRACUSE UNIV NY DEPT OF MECHANICAL AND AEROSPACE E--ETC F/G 9/5
RECTANGULAR FLAT-PACK LIDS UNDER EXTERNAL PRESSURE: IMPROVED FO--ETC(U)
JUN 79 C LIBOVE F30602-78-C-0083
UNCLASSIFIED MAE-1233-T1 RADC-TR-79-138 NL

| OF |
AD
A072421

END
DATE
FILMED
9-79
DDC

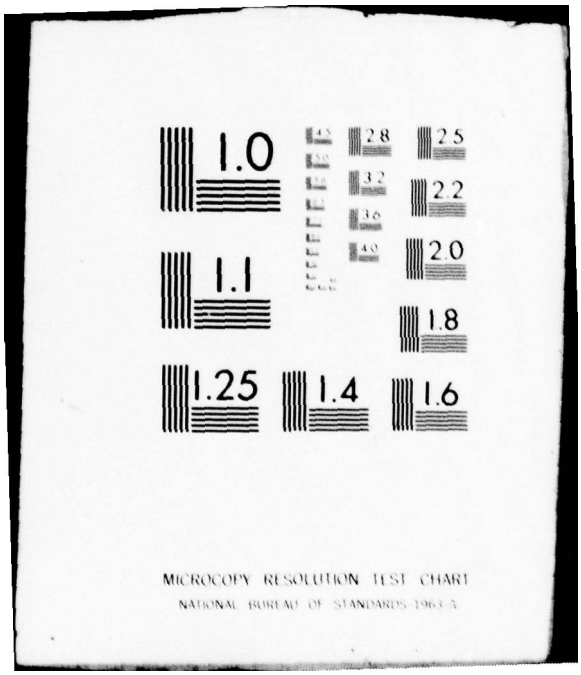
1.0
1.1
1.25
1.4
1.6
2.8
3.2
3.6
4.0
2.5
2.2
2.0
1.8
MICROCOPY RESOLUTION TEST CHART
NATIONAL BUREAU OF STANDARDS 1963-A

RADC-TR-79-138
Final Technical Report
June 1979

LEVEL II

RECTANGULAR FLAT-PACK LIDS UNDER EXTERNAL PRESSURE: IMPROVED FORMULAS FOR SCREENING AND DESIGN (REVISED)

Syracuse University

Charles Libove

ROME AIR DEVELOPMENT CENTER
Air Force Systems Command
Griffiss Air Force Base, New York 13441

This report has been reviewed by the RADC Information Office (OI) and is releasable to the National Technical Information Service (NTIS). At NTIS it will be releasable to the general public, including foreign nations.

RADC-TR-79-138 has been reviewed and is approved for publication.

APPROVED: Peter F. Manno

PETER F. MANNO
Project Engineer

APPROVED: Joseph J. Nakesky

JOSEPH J. NAKESKY
Chief, Reliability & Compatibility Division

FOR THE COMMANDER: John P. Huss

JOHN P. HUSS
Acting Chief, Plans Office

If your address has changed or if you wish to be removed from the RADC mailing list, or if the addressee is no longer employed by your organization, please notify RADC (RBRM), Griffiss AFB NY 13441. This will assist us in maintaining a current mailing list.

Do not return this copy. Retain or destroy.

UNCLASSIFIED

SECURITY CLASSIFICATION OF THIS PAGE (When Data Entered)

REPORT DOCUMENTATION PAGE

READ INSTRUCTIONS BEFORE COMPLETING FORM

1. REPORT NUMBER: RADC-TR-79-138	2. GOVT ACCESSION NO.
3. RECIPIENT'S CATALOG NUMBER	
4. TITLE (and Subtitle): RECTANGULAR FLAT-PACK LIDS UNDER EXTERNAL PRESSURE: IMPROVED FORMULAS FOR SCREENING AND DESIGN (REVISED)	5. TYPE OF REPORT & PERIOD COVERED: Final Technical Report
	6. PERFORMING ORG. REPORT NUMBER: MAE-1233-T1
7. AUTHOR(s): Charles Libove	8. CONTRACT OR GRANT NUMBER(s): F30602-78-C-0083
9. PERFORMING ORGANIZATION NAME AND ADDRESS: Syracuse University, Department of Mechanical & Aerospace Engineering, Syracuse NY 13210	10. PROGRAM ELEMENT, PROJECT, TASK AREA & WORK UNIT NUMBERS: 61102F, 2306J4P2
11. CONTROLLING OFFICE NAME AND ADDRESS: Rome Air Development Center (RBRM), Griffiss AFB NY 13441	12. REPORT DATE: June 1979
	13. NUMBER OF PAGES: 88
14. MONITORING AGENCY NAME & ADDRESS (if different from Controlling Office): Same	15. SECURITY CLASS. (of this report): UNCLASSIFIED
	15a. DECLASSIFICATION/DOWNGRADING SCHEDULE: N/A

16. DISTRIBUTION STATEMENT (of this Report)

Approved for public release; distribution unlimited.

17. DISTRIBUTION STATEMENT (of the abstract entered in Block 20, if different from Report)

Same

18. SUPPLEMENTARY NOTES

RADC Project Engineer: Peter F. Manno (RBRM)

19. KEY WORDS (Continue on reverse side if necessary and identify by block number)

Flat Packs	External pressure
Lids	Microelectronic packaging
Screening	Mechanical integrity
Hermeticity	
Seal integrity	

20. ABSTRACT (Continue on reverse side if necessary and identify by block number)

Earlier work is improved and extended to provide formulas for the maximum tensile stress in the lid-to-wall seal, the maximum lid deflection, and the lid collapsing pressure for a rectangular flat-pack under external pressure. It is shown how these formulas can facilitate (a) the proper design of the package so that it will retain its hermeticity and serviceability under a given screening pressure and (b) the selection of a proper pressure to use in the hermeticity screening of an already designed package. Information is (Cont'd)

DD FORM 1 JAN 73 1473

UNCLASSIFIED

SECURITY CLASSIFICATION OF THIS PAGE (When Data Entered)

Item 20 (Cont'd)

also given on the approximate equivalence of external pressure and centrifuge acceleration in regard to the seal stresses and lid behavior. Finally, experimental data on package hermeticity are presented which tend to confirm the validity of the main hypotheses of the present work.

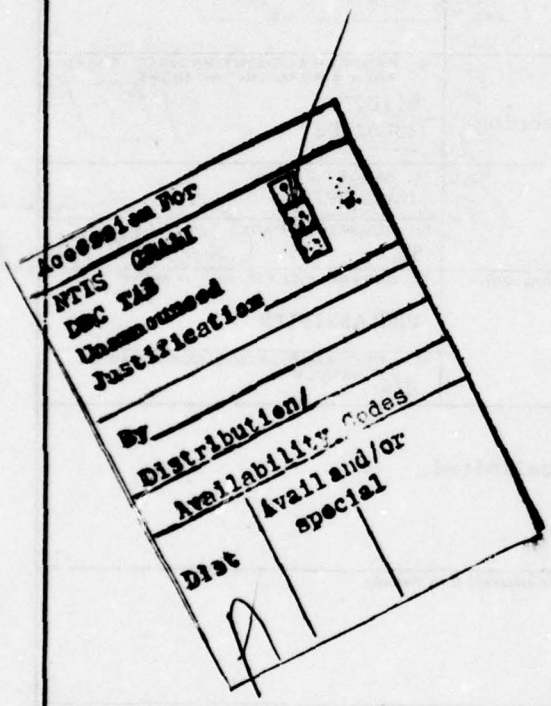

CONTENTS

EVALUATION

The objective of this effort was to develop and verify mathematical relationships to theoretically assess the mechanical stresses induced in large microcircuit packages under various environmental conditions.

As a result of this program, earlier work published in RADC-TR-76-291 has been improved and extended to provide formulas for the maximum tensile stress in the lid-to-wall seal, the maximum lid deflection, and the lid collapsing force for a rectangular flat-pack under external pressure. Some of the main improvements on the previous work includes a more thorough consideration of lid plasticity, especially as a limiting factor in the transfer of bending moment from the lid to the wall through the seal, and the inclusion of lids with thinned edges.

The data and information base established by this effort will be used by the Air Force to establish effective test levels as a function of package size and material and also by part manufacturers as design guidelines. The models and relationships which have been developed will be further verified by experimentation and will be considered in formulating revised screening requirements for MIL-STD-883, "Test Methods and Procedures for Microelectronics," Method 5008 and the package related tests of Method 5005.4.

Peter F. Manno

PETER F. MANNO
Project Engineer

RECTANGULAR FLAT-PACK LIDS UNDER EXTERNAL PRESSURE: IMPROVED FORMULAS FOR SCREENING AND DESIGN (REVISED)*

By Charles Libove

Professor of Mechanical and Aerospace Engineering
Syracuse University

I. SUMMARY

Earlier work is improved and extended to provide formulas for the maximum tensile stress in the lid-to-wall seal, the maximum lid deflection, and the lid collapsing pressure for a rectangular flat-pack under external pressure. It is shown how these formulas can facilitate (a) the proper design of the package so that it will retain its hermeticity and serviceability under a given screening pressure, and (b) the selection of a proper pressure to use in the hermeticity screening of an already designed package. Information is also given on the approximate equivalence of external pressure and centrifuge acceleration in regard to the seal stresses and lid behavior. Finally, experimental data on package hermeticity are presented which tend to confirm the validity of the main hypotheses of the present work.

II. INTRODUCTION

External pressure, per Method 1014.2 of Reference 1, is generally accepted as a means of screening out non-hermetic or potentially non-hermetic microelectronic packages. Knowing that this is the screening device

*The original version of this report was published as RADC-TR-76-291, September 1976 (AD-A025625). The present version differs from the original mainly in its more thorough consideration of lid plasticity and the inclusion of lids with thinned edges.

to be employed, the designer and the user of such packages are faced then with the following two questions, respectively:

(a) Given the screening pressure to which the package will be subjected, what should the design features of the package be in order that a seal of good quality will retain its hermeticity under that pressure?

(b) Given a package that is already designed and available, what screening pressure should be used in order to weed out (i.e., destroy the hermeticity or aggravate the non-hermeticity of) those seals at the low end of the quality spectrum?

In Reference 2a simple formulas and charts were developed as an aid in answering these two questions for rectangular flat-packs. The work of Reference 2a was limited to the case in which the package walls were of constant thickness and material and the lid-to-wall seal extended across the entire thickness of the top of the wall. In Reference 2b this work was extended to include walls whose thickness and materials might vary from top to bottom and seals whose widths are narrow compared to the wall thickness at the top of the wall.

In the first version of the present report (Reference 3) some improvements and additions were made to the previous work (References 2a and 2b). They included: (a) more reasonable definitions of the length and width of the package lid, (b) more reasonable assumptions regarding the elastic restraint furnished to the package walls by the base, (c) more complete data on lid deflections, (d) formulas for the ultimate strength of the lid under external pressure, and (e) experimental data on package hermeticity tending to validate the main hypotheses.

The present version incorporates two further improvements: (f) a more complete consideration of lid plasticity, especially as a limiting factor in the transfer of bending moment from the lid to the wall through the seal,

and (g) the inclusion of lids with thinned edges. Thus, the present report supersedes References 2a, 2b and 3, except for certain derivations in Reference 2a related to the present figures 7, 8 and 14. These derivations are not repeated in the present work.

The symbols to be used are defined where first introduced, and the definitions are also compiled in Appendix A for ease of reference.

Acknowledgement.- This report was written under Contract No. F30602-78-0083, Task No. PRN-8-5165, with the Air Force System Command's Rome Air Development Center, Griffiss Air Force Base, New York.

III. DESCRIPTION OF PACKAGES

The package is rectangular, as shown in Figure 1, with the cavity having width a, length b, and height h. The dimensions a and b are measured at the top of the cavity, and a is the shorter of the two if they are unequal. The dimension h is assumed to be small compared to b.

If ceramic, the lid is assumed to have a constant thickness t in the region above the cavity and to be no thinner than t in the edge regions above the walls. If metallic, the lid is assumed to have a constant thickness t in the region above the cavity and is allowed to have a smaller thickness t_e in the edge strips above the walls; if the lid does not have thinned edges, t_e should be replaced by t in the formulas to be developed.

The Young's modulus E (modulus of elasticity) and the Poisson's ratio ν of the lid material are assumed to be known. For most materials ν can be taken as 0.3 with little error. Knowing E, t and ν, one can compute the elastic "plate flexural stiffness" D of the lid as follows:

$$D = Et^3/[12(1-\nu^2)] \qquad (1)$$

The basic flexural strength of the lid is assumed to be known in terms of its ultimate bending moment per unit width, which will be designated as m in the interior and m_e in the edge regions, with the latter designation being pertinent only to metallic lids with edge zone thickness t_e smaller than the main thickness t. These ultimate bending moments per unit width can be computed from the bending modulus of rupture σ_b of the material via the formulas

$$m = \sigma_b t^2/6 \qquad m_e = \sigma_b t_e^2/6 \qquad (2)$$

By means of tests on cantilever strips cut from commercially available Kovar lids, the writer has estimated σ_b for such lids to be 107,000 psi with a coefficient of variation of 8 percent. For ceramic lids the value of σ_b can be obtained from the manufacturer's literature, where it is sometimes referred to as the "flexural strength" of the material.

There are different physical actions associated with the development of the ultimate bending moment, depending upon whether the lid is a ductile metal, like Kovar, or a brittle ceramic. In the former case, m and m_e are equal to the fully plastic bending moments per unit width, and they are associated with the development of very high curvatures without any fracture of the material. In the latter case, m is the bending moment per unit width at which fracture occurs, and there is little or no plastic deformation preceding the fracture.

Two kinds of wall construction will be assumed, namely "uniform" and "stepped," as illustrated in Figures 2(a) and (b). In the former, which is

typical of an all metal package, the material and the thickness w are constant along the entire height of the wall. In this case E_w and ν_w will denote the Young's modulus and Poisson's ratio of the wall material and

$$D_w \equiv E_w w^3/[12(1-\nu_w^2)] \qquad (3)$$

will denote its plate flexural stiffness. In the stepped wall, which is illustrated in Figure 2(b), the material and/or the thickness are only piece-wise constant. In such a wall, w, w_1, w_2, ..., will denote the thicknesses of the several segments, starting from the top. E_w, E_1, E_2, ..., will denote their respective Young's moduli; ν_w, ν_1, ν_2, ..., their Poisson's ratios; and D_w, D_1, D_2, ..., their plate flexural stiffnesses, defined as follows:

$$D_w \equiv \frac{E_w w^3}{12(1-\nu_w^2)}, \quad D_1 \equiv \frac{E_1 w_1^3}{12(1-\nu_1^2)}, \quad D_2 \equiv \frac{E_2 w_2^3}{12(1-\nu_2^2)}, \quad \ldots \qquad (4)$$

The top of the top segment of the wall will have a height above the base that is equal to h, the depth of the cavity. The heights of the tops of the remaining segments above the base will be denoted by h_1, h_2, ..., respectively, as indicated in Figure 2(b). In a typical three-segment stepped wall, like the one shown in Figure 2(b), the top segment might be a metal seal frame and the other two segments would be of glass. All four walls are assumed to be identical in construction and cross section.

Two kinds of lid-to-wall seal will be considered: the "wide seal" and the "narrow seal," which are illustrated in Figure 3. In the former, the seal width w_s is essentially equal to the thickness w of the top of the wall. This kind of seal would result typically from the use of a solder

preform. In the narrow seal, which might result from an electrical seam welding process, the seal width w_s is much smaller than w, and the seal is confined to the outer limits of the lid-wall interface. In such a seal, e will denote the distance from the inner edge of the wall top to the middle of the seal width (see Figure 3(b)).

IV. MAIN HYPOTHESES

The following assumptions are the main basis of the present work:

(a) Under hydrostatic external pressure, the lid may be regarded as a uniformly loaded rectangular plate, with width and length equal to the cavity dimensions a and b, and with edges elastically restrained against rotation by the walls of the package.

(b) The external pressure produces or enhances leakage paths in poor quality lid-to-wall seals mainly by the creation of tensile stresses in the outer portions of the seal that exceed the tensile strength of the seal material. (In poor quality seals, e.g., those containing voids or inclusions, this tensile strength will presumably be lower than in good quality seals.)

(c) Whether good or poor, the seal quality is reasonably uniform around the periphery of the lid, so that the damaging tensile stresses referred to in (b) need not be present along the entire periphery but may be localized at the middles of the longer sides.

Hypothesis (a) implies that we must evaluate the degree of elastic restraint furnished by the walls to the edges of the lid, and this is done in the next section.

V. ELASTIC RESTRAINT FURNISHED TO THE LID BY THE WALLS

The walls will be regarded as wide vertical beams of length (i.e., height) h, with the local rotation θ (in radians) at the upper end proportional to the local intensity M of the bending moment per unit width

exerted upon the wall by the lid as it flexes under external hydrostatic pressure*. This relationship can be expressed as

$$M = k\theta \tag{5}$$

where k is a proportionality constant. The value of k depends upon the moment M_b per unit width which the base of the package exerts upon the lower end of the wall (see Figure 4(a)). In what follows we will make the simplifying assumption that $M_b = M$, as shown in Figure 4(b).**

Assuming $M_b = M$, and analyzing the wall as a wide beam of length h, we arrive at the following formula for k:

$$k = \alpha \frac{D_w}{h} \tag{6}$$

where α is a dimensionless constant whose value depends on the nature of the wall. If the wall is uniform, as in Figure 2(a),

$$\alpha = 2 \tag{7a}$$

If the wall is a three-segment stepped wall, as in Figure 2(b),

---

*The lid exerts a vertical force as well as a moment upon the inside edge of the top of the wall. The small additional bending of the wall due to this force is being neglected.

**This assumption is correct in the case of a uniform wall with the base and lid identical, for then a horizontal plane of symmetry exists at the mid-height of the package. It is also nearly correct in the case of short stubby walls (uniform or not) that effectively clamp the edges of the lid and base (which need not be identical). This is because the bending moments along the edges of a clamped rectangular plate under uniform pressure are virtually independent of the plate material and thickness, depending almost entirely on the pressure and the dimensions a and b (see Table 35 of Reference 4); thus the lid and base, having the same pressure and being about the same size, will have nearly identical distributions of bending moments around their edges when the latter are in a clamped or nearly clamped state. Since most packages fall fairly close to one or both of the two cases just described, the assumption $M_b = M$ is felt to be appropriate.

$$\alpha = \frac{2}{\frac{D_w}{h^2}\left(\frac{h^2-h_1^2}{D_w} + \frac{h_1^2-h_2^2}{D_1} + \frac{h_2^2}{D_2}\right)} \tag{7b}$$

For an n-segmented stepped wall,

$$\alpha = \frac{2}{\frac{D_w}{h^2}\left(\frac{h^2-h_1^2}{D_w} + \frac{h_1^2-h_2^2}{D_1} + \frac{h_2^2-h_3^2}{D_2} + \ldots + \frac{h_{n-1}^2}{D_{n-1}}\right)} \tag{7c}$$

Setting $D_1 = D_2 = \ldots = D_w$ in Eqs. (7b) and (7c) reduces them to (7a), as it should.

For later use we now introduce a dimensionless wall stiffness parameter, K, which is essentially a measure of the ratio of the wall flexural stiffness to the lid flexural stiffness. K is defined as follows:

$$K \equiv \frac{4}{\pi^2}\frac{k}{(D/a)} = \frac{4}{\pi^2}\frac{a}{h}\frac{D_w}{D}\alpha \tag{8a}$$

If the Poisson's ratios ν and ν_w are equal, this definition reduces to

$$K = \frac{4}{\pi^2}\frac{a}{h}\frac{E_w}{E}\left(\frac{w}{t}\right)^3\alpha \tag{8b}$$

In graphs to be given later, certain quantities are plotted as functions of arctan K, rather than as functions of K. Figure 5 will permit an easy conversion from K to arctan K. For most packages arctan K will be fairly close to the upper limit of $\pi/2$, or 1.57, implying that the edges of the lid are very close to being clamped by the walls.

VI. FORMULAS FOR MAXIMUM TENSILE STRESS IN THE SEAL

A. Linearly Elastic Lid.- Under the action of a uniform gage pressure p (psi), reactions will develop along the edges of the lid, as

depicted in Figure 6. These will include bending moments of varying intensity M (in.-lb per in.), due to the restraint against rotation furnished by the walls, and an effective vertical shear of varying intensity V (lb per in.). The maximum values of M and V occur at the middle of the long side and, as long as the lid is linearly elastic (i.e., obeys Hooke's Law), can be expressed as

$$M_{max} = n_1 \cdot pa^2 \tag{9}$$

$$V_{max} = n_2 \cdot pa \tag{10}$$

where n_1 and n_2 are functions of the elastic restraint parameter K and the aspect ratio b/a of the lid. The values of n_1 and n_2 associated with any given configuration can be obtained from Figures 7 and 8, respectively.

The maximum tensile stress S_{max} in the seal is most likely to occur at the middle of the long side, where the bending moment transmitted from the lid to the wall is a maximum. At this location the bending moment M_{max} and vertical shear V_{max} are transferred to the edge strip of the cover directly over the wall, as shown in Figure 9.**. The edge strip transfers

*In Figure 7 the data for a clamped plate ($K = \infty$, arctan $K = \pi/2$) are taken from Table 35 of Reference 4. All other data in this figure are based on the analysis in Appendix A of Reference 2a. In Figure 8 the data for a simply supported plate (arctan $K = 0$) are from Table 8 of Reference 4. The data for a clamped plate (arctan $K = \pi/2$) are based on the analysis in Appendix B of Reference 2a. The curves for elastically restrained plates (arctan K = .4, .8, 1.2) were inserted by interpolation, assuming a linear variation of n_2 with respect to arctan K, which is approximately the variation obtained for n_1. In view of the small change in n_2 in going from simple support to clamping (around 6% at the most) and the small role that n_2 will play in the subsequent development, the linear interpolation employed in Figure 8 is considered acceptable.

**Recall that for analytical purposes we are considering the lid to end at the inner edges of the wall.

these in turn to the top of the wall, along with the force pw per unit length due to hydrostatic pressure p acting at the top of the edge strip. Thus, the edge strip is essentially a loading device to transfer the forces shown in Figure 9 to the wall below it.

The states of stress assumed to be developed at the top of the wall, as a result of the forces applied to it by the edge strip in the middle of the long side, are shown in Figure 10. In the case of a wide seal we are assuming a linear variation of normal stress across the thickness of the wall. In the case of a narrow seal we assume instead a uniform tensile stress in the seal area together with a concentrated compressive line load along the inner edge of the wall. In both cases the maximum tensile stress S_{max} in the seal material occurs at the outside edge.

The stress distributions of Figure 10 must be statically equivalent to the loading of Figure 9. From this equivalence one can deduce the following expressions for the maximum tensile stress in the seal:

$$S_{max} = \left(M_{max} + V_{max}\frac{w}{2}\right)\frac{6}{w^2} - \left(p + \frac{V_{max}}{w}\right) \qquad (11a)$$

in the case of a wide seal (Figure 10(a)), and

$$S_{max} = \frac{M_{max} - \frac{1}{2}pw^2}{w_s e} \qquad (11b)$$

in the case of a narrow seal (Figure 10(b)). Substituting for M_{max} and V_{max} their known values from Equations (9) and (10), we obtain the following formula for computing S_{max}:

$$S_{max} = p\left(\frac{a}{w}\right)^2 n \qquad (12)$$

where

$$n = 6n_1 + 2n_2 \frac{w}{a} - \left(\frac{w}{a}\right)^2 \qquad (13a)$$

in the case of a wide seal, and

$$n = \left[n_1 - \frac{1}{2}\left(\frac{w}{a}\right)^2\right] \frac{w^2}{ew_s} \qquad (13b)$$

in the case of a narrow seal. In extreme cases Equation (12) will give negative values of S_{max}, implying that no amount of external pressure can produce tension in the seal.

Brittle materials, such as ceramics, obey Hooke's law reasonably well up to the point of fracture. Thus, Equation (12), which is based upon Hooke's law, may be assumed to be valid for ceramic lid packages as long as the pressure p is less then the lid collapsing pressure $p_{ultimate}$ discussed in Section VII.

B. Inelastic Lid.- Equation (9) is based on Hooke's law and it therefore predicts a linear relationship between M_{max} and p, which is represented by the line OBEA in Figure 11. In the case of a brittle material lid this line may be considered valid for all pressures up to the point of fracture. If the lid is of a ductile metal, however, at some point, represented by B in Figure 11, the pressure will become high enough to produce plastic (i.e., inelastic) behavior. The lid will not fracture, but the graph of M_{max} versus p will depart from the straight line, and M_{max} will approach the fully plastic bending moment m_e asymptotically along a curve such as OBCD. The determination of this curve is a difficult problem in elasto-plastic plate analysis. We shall avoid this problem by simply approximating the curve OBCD by the two straight-line segments OE and ED. That is, Equation (9) will be considered valid as long as its right side, $n_1 pa^2$, is less than m_e, and Equation (9) will be replaced by

$$M_{max} = m_e \tag{14}$$

if $n_1 pa^2$ equals or exceeds m_e. Equation (10) is also based on Hooke's law, and its validity will therefore also break down at the pressure associated with point B of Figure 11. We shall ignore this, however, and continue to use Equation (10) for all pressures, on the ground that V_{max} generally plays a smaller role than M_{max} in producing stress in the seal and we therefore do not need to know it as precisely. Thus, the sole effect of lid plasticity in our considerations will be to replace Equation (9) by (14) if $n_1 pa^2$ equals or exceeds m_e; that is, if

$$p \geq m_e/n_1 a^2 \equiv p_t \tag{15}$$

We shall call the right side of this inequality the transition pressure and, as indicated, represent it by the symbol p_t. It is the pressure associated with point E in Figure 11. The corresponding value of S_{max} we shall call the transition stress and represent it by S_{max_t}. S_{max_t} can be evaluated by substituting the transition pressure $p_t = m_e/n_1 a^2$ for p in Equation (12), with the result

$$S_{max_t} = m_e n/w^2 n_1 \tag{16}$$

When the inequality (15) is satisfied, we may compute S_{max} from Equations (11) by substituting m_e for M_{max} and the right side of Equation (10) for V_{max}. The result is

$$S_{max} = \frac{6m_e}{w^2} + p(2n_2 \frac{a}{w} - 1) \tag{17}$$

for a wide seal, and

$$S_{max} = \frac{m_e}{w_s e} - p\left(\frac{w^2}{2w_s e}\right) \tag{18}$$

for a narrow seal.

Equations (17) and (18) show that now the worst case (i.e., the largest positive S_{max}) does not necessarily occur at the highest pressure. This is because the p term in Equation (18) is always negative and the p term in Equation (17) is negative if $2n_2 \frac{a}{w} - 1$ is negative. Thus, increasing p can cause a reduction in S_{max}. To obtain "worst-case" formulas, we must replace p in Equation (18) by the lowest value it can have and still satisfy condition (15), that is, by the transition pressure p_t; and we must make the same replacement in Equation (17) if $2n_2 \frac{a}{w} - 1$ is negative. Consequently, given any existing pressure p which satisfies (15), the maximum seal tension produced <u>in the course of applying that pressure</u> (not necessarily the seal tension <u>at</u> that pressure) is:

$$S_{max} = \text{the larger of} \begin{cases} \dfrac{6m_e}{w^2} + p\left(2n_2 \dfrac{a}{w} - 1\right) \\ \text{and} \\ \dfrac{6m_e}{w^2} + \dfrac{m_e}{n_1 a^2}\left(2n_2 \dfrac{a}{w} - 1\right) \end{cases} \tag{19a}$$

for a wide seal; and

$$S_{max} = \frac{m_e}{w_s e} - \frac{m_e}{n_1 a^2}\left(\frac{w^2}{2w_s e}\right) = \frac{m_e}{w_s e}\left[1 - \frac{1}{2n_1}\left(\frac{w}{a}\right)^2\right] \tag{19b}$$

for a narrow seal. Equations (19) can give negative values for S_{max}, which means that the given pressure has produced no tension in the seal. Like Equation (12), they are limited to pressures below the lid collapsing pressure $p_{ultimate}$ discussed in Section VII.

C. Summary of Formulas for S_{max}.- The formulas for S_{max} developed in the two preceding sections are summarized in Table 1.

D. Application to Design.- The formulas of Table 1 can be of use both to the designer, whose objective is to design a package that will remain hermetic under a specified screening pressure p, and the user, whose objective is to select an appropriate screening pressure p that will worsen or destroy the hermeticity of packages with poor quality seals.

Considering the first designer, let us suppose that he knows the sealing material to be used and has a value for the allowable tensile stress S_{all} of that material. Then his criterion for a satisfactory lid-to-wall seal design, from the point of view of retaining hermeticity under a given external screening pressure p, should be that S_{max}, as given by the appropriate box of Table 1, be less than S_{all}. That is,

$$S_{max} \leq S_{all} \tag{20}$$

In selecting S_{all} the designer should of course be conservative. If S_{all} is taken as the median tensile strength of the sealing material, then packages designed on the basis of the equality sign in Equation (20) will have a failure rate of approximately 50% even if properly sealed. (The failure rate will be still higher for a mixture of properly and improperly sealed packages.) On the other hand, if the designer selects for S_{all} the lowest 1-percentile value of the material strength, then he should expect only 1% failure rate for properly sealed packages designed on the basis of Equation (20) with the equality sign. The designer should also consider the possibility of the deposited sealing material or its interfacial compounds having a different tensile strength than the bulk sealing material.

Table 1.- Summary of Formulas for Maximum Seal Stress, S_{max}

	Linearly Elastic Lid		Inelastic Lid
	Brittle Material	Ductile Material and $p<m_e/n_1a^2 \equiv p_t$	Ductile Material and $p>m_e/n_1a^2 \equiv p_t$
Wide Seal	$S_{max} = p(\frac{a}{2})^2 n$ where $n = 6n_1 + 2n_2 \frac{w}{a} - (\frac{w}{a})^2$ [Eqs. 12 and 13(a)]		S_{max} = the larger of $\frac{6m_e}{w^2} + p(2n_2 \frac{a}{w} - 1)$ and $\frac{6m_e}{w^2} + \frac{m_e}{n_1a^2}(2n_2 \frac{a}{w} - 1)$ [Eq. 19(a)]
Narrow Seal	$S_{max} = p(\frac{a}{w})^2 n$ where $n = [n_1 - \frac{1}{2}(\frac{w}{a})^2] \frac{w^2}{ew_s}$ [Eqs. 12 and 13(b)]		$S_{max} = \frac{m_e}{w_s e}[1 - \frac{1}{2n_1}(\frac{w}{a})^2]$ [Eq. 19(b)]

There is one special precaution to be observed in applying Equation (20) to a stepped-wall package (Figure 2(b)). In such a package the uppermost wall segment is typically a metal seal frame, while the segment below it is of glass. In that case, the critical seal could be the glass-metal interface (or the glass itself) at the underside of the seal frame, rather than the metal-to-metal bond at the top of the seal frame. Therefore, the designer should be sure that the inequality in Equation (20) is satisfied for both seals - the usually wide (but possibly narrow) one at the top of the seal frame, with S_{all} based on the tensile strength of the sealant there; and the wide seal of width w at the underside of the seal frame, with S_{all} based on the tensile strength of the glass.

It could happen that the designer has very little data on the distribution of tensile strength values for the sealing material, or even on the mean strength, but he does know that a certain previously designed similar package, designated as I, when properly sealed with the same material had an acceptable failure rate F under a screening pressure of p_I. Then in order for the new package, designated as II, to have a failure rate no greater than F when properly sealed and subjected to its screening pressure p_{II}, he should so design package II that its S_{max} is no greater than that of package I. Thus, his criterion for a satisfactory design of package II should be

$$(S_{max})_{II} \leq (S_{max})_{I} \tag{21}$$

where both S_{max}'s are taken from Table 1, but not necessarily from the same box of that table.

E. Application to Screening.- Turning now to the user of an already designed package, let us first suppose that he has a minimum acceptable value, S_{accept}, for the tensile strength of the seal, and he wants to be sure of rejecting all packages with seal strengths less than that. Then he should select a screening pressure p such that the S_{max} given by Table 1 is equal to or greater than S_{accept}, or, if that cannot be accomplished, a screening pressure p that will make S_{max} as large as possible.

In the case of a ductile material lid, the procedure for accomplishing this depends upon whether S_{accept} is less than or greater than the transition stress S_{max_t} defined by Equation (16). If $S_{accept} < S_{max_t}$, the elastic formula (12) applies. Replacing S_{max} in this formula by S_{accept}, and solving for p, we obtain

$$p = S_{accept}\left[\left(\frac{a}{w}\right)^2 n\right]^{-1} \tag{22}$$

as the appropriate screening pressure. On the other hand, if $S_{accept} > S_{max_t}$, Equations (19) apply. Then for a wide seal with $2n_2 \frac{a}{w} - 1$ positive, we may equate the top expression of (19a) to S_{accept} and solve for p to obtain the following formula for the appropriate screening pressure:

$$p = \left(S_{accept} - \frac{6m_e}{w^2}\right)\left(2n_2 \frac{a}{w} - 1\right)^{-1} \tag{23}$$

In the case of a narrow seal, or a wide seal with $2n_2 \frac{a}{w} - 1$ negative, it is not possible to achieve $S_{max} = S_{accept}$ when $S_{accept} > S_{max_t}$, for in those cases S_{max_t} is also the largest achievable value of S_{max}. Then we must settle for a screening pressure that will give S_{max} as large a value as possible; since that value is S_{max_t}, the required pressure is

$$p = p_t = m_e/n_1 a^2 \qquad (24)$$

In the case of a ceramic lid, linearly elastic behavior will be assumed in the lid up to fracture. Thus, Equation (22) may be used in such a case as long as the screening pressure it provides is less than the lid collapsing pressure $p_{ultimate}$ discussed in Section VII.

The screening pressure formulas developed in this section are summarized in Table 2. The pressures therein should be regarded as minimums. Larger pressure, applied through stepwise increments, can be used as long as they are below $p_{ultimate}$ and do not cause undesirably large lid deflections. The effect of using a pressure that is higher than the one specified in the table is to enlarge the portion of the lid periphery in which the extreme-fiber seal stress exceeds S_{accept} or has equalled S_{max_t}. The use of larger pressures may be particularly advisable when the lid is ductile, in view of the fact that the simplified curve OBED of Figure 11, on which the tabulated formulas are based, tends to over-estimate M_{max}.

Table 2.- Summary of Formulas for Appropriate Screening Pressure

Brittle Lid	Ductile Lid			
	$S_{accept} \leq S_{max_t}$	$S_{accept} > S_{max_t}$		
		Wide Seal		Narrow Seal
		$2n_2 \frac{a}{w} - 1 \geq 0$	$2n_2 \frac{a}{w} - 1 < 0$	
$p = \frac{S_{accept}}{(\frac{a}{w})^2 n}$ [Eq. (22)]		$p = \frac{S_{accept} - \frac{6m_e}{w^2}}{2n_2 \frac{a}{w} - 1}$ [Eq. (23)]		$p = \frac{m_e}{n_1 a^2}$ [Eq. (24)]

In order to use the formulas in Table 2, one must decide on a value of the minimum acceptable seal strength, S_{accept}. It is conceivable that the screener of a package will not have enough information about the sealing material to be able to specify a value for S_{accept}, but he might know that in the past a certain pressure p_I was considered suitable for screening a certain package, designated as package I, that employed the same sealing material as the package now under consideration, which will be designated as package II. Then the S_{max} produced in package I by its screening pressure p_I should be an acceptable maximum seal stress in package II. Thus, the following rule can be used to arrive at a value of S_{accept} for package II:

$$(S_{accept})_{II} = (S_{max})_{I} \text{ produced by } p_I \tag{25}$$

where the quantity on the right side is obtained from the appropriate formula of Table 1.

VII. LID COLLAPSING PRESSURE

It is important, in both screening and design, to be able to estimate the lid collapsing pressure $p_{ultimate}$, and in this section formulas are presented to facilitate making such an estimate. In presenting these formulas we consider separately lids of a brittle material, such as ceramic, and lids of a ductile material, such as Kovar, since the mechanism of collapse is different for both types.

A. Brittle-Material Lids.- For a lid made of perfectly brittle material it could be assumed that fracture will occur when the calculated maximum tensile stress σ_{max} in the lid equals the ultimate tensile strength σ_t of the material. Ceramics employed for microelectronic

packaging may not, however, be perfectly brittle in flexure. This is evidenced by the fact that quoted values of the bending modulus of rupture σ_b (also called "flexural strength") of such ceramics are somewhat higher than the quoted values of σ_t (see Reference 8 for examples). Therefore it may be somewhat more realistic to take the following as a criterion of fracture or collapse of supposedly brittle-material lids:

$$\sigma_{max} = \sigma_b \tag{26}$$

In order to apply this criterion, one must have information on σ_{max} as a function of the applied pressure p. Information of this kind is presented in Figure 12, which is based mainly on Reference 6 and which takes into account large-deflection effects. Figure 12 gives σ_{max} through a dimensionless constant n_7 related to σ_{max} as follows:

$$\sigma_{max} = n_7 E \left(\frac{t}{a}\right)^2 \tag{27}$$

This relationship permits the collapse criterion (26) for brittle-material lids to be written as

$$n_7 = \frac{\sigma_b}{E} \left(\frac{a}{t}\right)^2 \tag{28}$$

The graphs of n_7 (Figure 12) require some discussion: Although data for n_1 are available for K values ranging from 0 to ∞ (arctan K ranging from 0 to $\pi/2$), data for n_7 are available only for the limiting cases of simple support (K = arctan K = 0) and clamping (K = ∞, arctan K = $\pi/2$). Therefore interpolation between a K = ∞ graph and a K = 0 graph of Figure 12 may sometimes be needed in estimating n_7. A linear interpolation based on arctan K, though non-rigorous, should be sufficiently accurate for

practical purposes; for most large flat-packs the assumption $K = \infty$ would also be suitable. A second difficulty associated with the estimation of n_7 derives from the fact that the large-deflection behavior of a plate is sensitive to whatever restraint the plate edges are under, in regard to their movement in the plane of the plate. Graphs (a) and (c) of Figure 12 assume that such restraint is negligible; these graphs are felt to be appropriate when the wall stretching stiffness (e.g., $E_w hw$ in the case of a uniform wall) is small compared to the lid stretching stiffness, Eat. Graphs (b) and (d), on the other hand, assume that the edges are free to curve inward but not to strain along their length; these graphs are more appropriate for cases in which the wall stretching stiffness ls large compared to the lid stretching stiffness. For most large flat-packs Figure 12(c) should be appropriate.

Let us denote by $p_{ultimate_1}$ the collapse pressure estimate obtained through the use of Equation (28) in conjunction with the graphs of Figure 12. Because of the above-discussed difficulties and uncertainties connected with the use of those graphs, there will always be some question as to the reliability of $p_{ultimate_1}$ as a true measure of the collapse pressure. It is therefore recommended that a second estimate, $p_{ultimate_2}$, be obtained by assuming σ_{max} to be the extreme-fiber stress at the edge of the lid in the middle of the long side, where, through Equation (9) and Figure 7, we have fairly accurate information about the bending moment as a function of both p and K in the small deflection régime. Accordingly, we write

$$\sigma_{max} = \frac{6M_{max}}{t^2} = \frac{6n_1 pa^2}{t^2} \tag{29}$$

then substitute this expression into Equation (26) and solve for p, to obtain

$$p_{ultimate_2} = \frac{\sigma_b}{6n_1} \left(\frac{t}{a}\right)^2 \tag{30}$$

as the second estimate of collapse pressure. Because it is based on a restricted search for σ_{max} (a search restricted to the middle of the long edge of the lid), $p_{ultimate_2}$ is likely to be an upper bound to the true collapse pressure. Therefore, it is advisable to select the smaller of $p_{ultimate_1}$ and $p_{ultimate_2}$ as the governing estimate of the collapse pressure of a brittle-material lid.

B. Ductile-Material Lids.- Collapse of ductile plates under lateral pressure is usually assumed to occur through the formation of plastic-hinge lines (yield lines). An approximate analysis of a ductile lid on this basis (Appendix B) leads to the following collapse pressure:

$$p_{ultimate} = n_8 \frac{2(m_e + m)}{a^2} \tag{31}$$

where

$$n_8 \equiv 4 + 3.2 \frac{a}{b} + 3.5 \left(\frac{a}{b}\right)^2 \tag{32}$$

and m_e and m are respectively the edge and interior fully plastic bending strengths of the lid. For a constant-thickness lid ($t_e = t$), m_e and m are equal. To facilitate the use of Equation (31) a graph of Equation (32) is plotted in Figure 13. Equation (31) is likely to be conservative, because the strengthening effect of membrane action was not considered in its derivation.

VIII. LID DEFLECTION

The maximum deflection δ_{max} of the lid under any pressure p will occur at the center of the lid. Both the designer and the user must concern themselves with this deflection, in order to insure that during any screening the lid will not come in contact with the contents of the package. In this section we present formulas and graphs for estimating δ_{max}. We consider separately the brittle-material and ductile-meterial lids. In the first case, plasticity (departure from Hooke's law) will play a negligible role; in the second case it will play a significant role.

A. Brittle-Material Lids.- An analysis based on the small-deflection theory of elastic plates is carried out in Appendix A of Reference 2a and leads to the following result:

$$\delta_{max} = n_4 \frac{pa^4}{D} = 12(1 - \nu^2) \frac{p}{E} \left(\frac{a}{t}\right)^3 an_4 \qquad (33)$$

where n_4 is the function of K and b/a plotted in Figure 14. With ν taken as 0.3, this formula reduces to

$$\delta_{max} = 10.92 \frac{p}{E} \left(\frac{a}{t}\right)^3 an_4 \qquad (34)$$

It is well known, however, that small-deflection theory tends to overestimate the deflection. Figure 15 therefore presents curves from which a correction factor n_5, based on large-deflection theory, can be estimated. (The graphs of Figure 15 are for the same four boundary conditions as those of Figure 12, and the earlier discussion of those boundary conditions is pertinent here as well.) With this correction factor included, the above formulas now read

$$\delta_{max} = 12(1-\nu^2)\,\frac{p}{E}\left(\frac{a}{t}\right)^3 a n_4 n_5 \simeq 10.92\,\frac{p}{E}\left(\frac{a}{t}\right)^3 a n_4 n_5 \qquad (35)$$

This equation can be considered valid for brittle-material lids at all pressures up to the lid-collapsing pressure $p_{ultimate}$.

B. Ductile-Material Lids.- For lids of a ductile material, like Kovar, Equation (35) will apply in the initial stages of pressure application. When the pressure becomes high enough, however, Hooke's law breaks down because of the initiation of plastic flow in the material. As the pressure is increased beyond this point, the regions of plastic deformation are enlarged and Equation (35) becomes increasingly in error on the low side. Finally, the collapse pressure $p_{ultimate}$ is reached, at which the lid deflections increase virtually without limit.

The precise determination of lid deflections in a ductile lid beyond the range of validity of Hooke's law is a difficult computational task which will not be attempted here. Instead, a simplified model of the lid's behavior will be proposed which will lead to an approximate estimate of the central deflection with very little computational effort.

The proposed model breaks the entire load-central deflection history into three régimes which are represented by the curve segments OA, AB and BC of Figure 16. The first segment, OA, corresponds to linearly elastic material behavior and it is the initial portion of the load-deflection curve OG defined by Equation (35). The second segment, AB, is part of the curve DE, which is the pressure-versus-deflection curve of a simply supported linearly elastic plate subjected to increasing pressure p in conjunction with a constant and uniform restraining moment of m_e per unit width along its periphery. And the third segment, BE, represents the indeterminate deflections occurring under the collapse pressure $p_{ultimate}$.

Thus, the model assumes an abrupt transition at A from a truly elastic behavior (OA) to a regime AB in which the fully plastic bending moment is developed all around the boundary while the interior of the lid still behaves elastically, then another abrupt transition at B to a regime BC of fully developed interior as well as exterior yield lines creating a collapse mechanism. In actuality, gradual transitions occur from one regime to the next, as suggested by the dashed curve, but such transitions are not included in the present model.

In order to make use of the proposed model, one must have an equation for the middle portion, AB, of the graph of pressure versus deflection. On the basis of linear elastic small-deflection plate theory (Figure 14 of the present paper and pp. 162-165 of Reference 4), the following equation can be derived for the line DE of which AB is a part:

$$\delta_{max} = 12(1-\nu^2)\,\frac{p}{E}\left(\frac{a}{t}\right)^3 a n_4(0) - \frac{m_e a^2}{D}\, n_9 \qquad (36)$$

where $n_4(0)$ is the value of n_4 from Figure 14 for $K = 0$, and n_9 is the following functions of b/a:

$$n_9 = \frac{4}{\pi^3} \sum_{m=1,3,5..}^{\infty} \frac{\sin(m\pi/2)}{m^3} \left[1 - \operatorname{sech}\left(\frac{m\pi}{2}\,\frac{b}{a}\right)\right] \qquad (37)$$

The first term on the right side of Equation (36) is the central deflection of a simply supported plate under a pressure p, and the second term is the diminution of that deflection due to the fully plastic restraining moment m_e along the boundary. Making use of Equation (1) we may rewrite Equation (36) as

$$\delta_{max} = \frac{12(1-\nu^2)a^2}{Et^3}\left[pa^2 n_4(0) - m_e n_9\right] \qquad (38)$$

and we note that for $\nu = 0.3$, $12(1-\nu^2)$ equals 10.92. To further facilitate the use of Equation (38), graphs of $n_4(0)$ and n_9 are given in Figures 17 and 18, respectively.

On the basis of the above discussion, we can now give the following rule for estimating the central deflection δ_{max} of a ductile-material lid:

For $p \leq p_{ultimate}$, δ_{max} is the larger of δ_{max_1}, δ_{max_2}, where δ_{max_1} is the deflection computed from Equation (33) or (34) and δ_{max_2} is the deflection computed from Equation (38). For $p > p_{ultimate}$, δ_{max} is arbitrarily large. (39)

IX. FLAT-PACKS IN A CENTRIFUGE

As part of the total screening process, packages are frequently spun in a centrifuge in such a way that the centrifugal force tends to push the lid into the cavity. As far as the lid alone is concerned, this centrifugal force is equivalent to a lateral pressure of Gtd, where

d = specific weight (weight per unit volume) of the lid material

t = thickness of lid

G = centripetal acceleration in units of g (acceleration of gravity)

If t is in inches and d in lbs per cubic inch, the formula

$$p_{equivalent} = Gtd \tag{40}$$

will give the effective pressure in psi due to a centrifuge acceleration of G g's. Alternatively, given any pressure p, we have from Equation (40) the following formula for the number of g's of centrifuge acceleration

equivalent to that pressure:

$$G_{equivalent} = \frac{p}{td} \tag{41}$$

As an example of the use of this formula, let us consider a lid of .030 in. thickness and .302 lb/in.^{3} specific weight and ask how many g's of centrifuge acceleration are equivalent to a lateral pressure of 30 psi. From Equation (41) we obtain the following answer:

$$G_{equivalent} = \frac{30}{(.030)(.302)} = 3310 \text{ (g's)} \tag{42}$$

By virtue of the equivalence relation (40), all the formulas and graphs of the preceding sections can be made to apply to a package in a centrifuge simply by replacing the symbol p everywhere by Gtd. In this way, for example, the following formula is obtained from Equation (35) for the central deflection of a linearly elastic lid of a package in a centrifuge:

$$\sigma_{max} = 10.92 \frac{Gtd}{E} \left(\frac{a}{t}\right)^3 a\, n_4\, n_5 \tag{43}$$

where n_5 is to be obtained from the graphs of Figure 15 with the abscissa labels therein changed to $Gtda^4/Et^4$. Similarly, Equation (12) gives the following formula for the maximum tensile stress in the seal when $Gtd < p_t$:

$$S_{max} = Gtd \left(\frac{a}{w}\right)^2 n \tag{44}$$

It should be noted, however, that the interaction among the base, the walls, and the lid is slightly different for a package in a centrifuge than for the same package under hydrostatic pressure. Therefore the values of α to be used in Equations (8) for evaluating K are no longer strictly as

given by Equations (7). The appropriate values of α depend on the manner in which the package is supported in the centrifuge.

Two possible types of support are illustrated in Figure 19. In the first, Figure 19(a), the package is supported only along its edges. The lid and the base then deflect in the same direction (rather than in opposite directions, as they would under hydrostatic pressure). If the base and lid are identical the bending moment intensity M_b acting upon the bottom of the wall will equal the bending moment intensity M acting upon the top of the wall, and both bending moments will have the same sense. If the base and lid are not identical, the equality of M_b and M does not hold; instead a reasonable assumption is

$$M_b = M\beta \tag{45}$$

where

$$\beta \equiv \frac{\text{mass of base}}{\text{mass of lid}} \tag{46}$$

and the base, like the lid, is considered to end where it meets the walls. Analyzing the wall as a wide beam under bending moments per unit width of M at the top and $M_b = M\beta$ at the bottom, both having the same sense, we arrive at the following formulas to replace (7a) and (7b), respectively:

$$\alpha = \frac{6}{2-\beta} \tag{47a}$$

$$\alpha = \frac{(6h^3/D_w)}{\left[-3\beta h\left(\frac{h^2-h_1^2}{D_w} + \frac{h_1^2-h_2^2}{D_1} + \frac{h_2^2}{D_2}\right) + (2\beta+2)\left(\frac{h^3-h_1^3}{D_w} + \frac{h_1^3-h_2^3}{D_1} + \frac{h_2^3}{D_2}\right)\right]} \tag{47b}$$

The replacement for Equation (7c) can be written by noting the pattern of the terms within parentheses in the denominator of Equation (47b) and extending it to n segments.

A more likely support condition is that illustrated in Figure 19(b). There the base is firmly bonded to a flat surface, producing an essentially clamped condition for the bottoms of the walls. The following formulas should then be used in place of (7a) and (7b), respectively:

$$\alpha = 4 \tag{48a}$$

α = Same expression as (47b), but with β defined by Equation (49) below, instead of Equation (46). (48b)

$$\beta \equiv \frac{3h\left(\frac{h^2-h_1^2}{D_w} + \frac{h_1^2-h_2^2}{D_1} + \frac{h_2^2}{D_2}\right) - 2\left(\frac{h^3-h_1^3}{D_w} + \frac{h_1^3-h_2^3}{D_1} + \frac{h_2^3}{D_2}\right)}{\left[6h^2\left(\frac{h-h_1}{D_w} + \frac{h_1-h_2}{D_1} + \frac{h_2}{D_2}\right) - 6h\left(\frac{h^2-h_1^2}{D_w} + \frac{h_1^2-h_2^2}{D_1} + \frac{h_2^2}{D_2}\right) + 2\left(\frac{h^3-h_1^3}{D_w} + \frac{h_1^3-h_2^3}{D_1} + \frac{h_2^3}{D_2}\right)\right]} \tag{49}$$

Equation (48b) reduces to (48a), as it should, when $D_2 = D_1 = D_w$. To obtain a replacement for Equation (7c) we generalize Equations (48b) and (49) to an n-segmented wall by noting the pattern of each parenthetical grouping of terms.

Equations (47) and (48) will generally lead to larger α's (stiffer walls) than those obtained under external pressure. Therefore, if the lid is already close to being clamped under external pressure (arctan K close

to $\pi/2$), there is no need to bother with the above refinements in the α calculation when going to a centrifuge environment.

X. NUMERICAL EXAMPLES

Here we pose and solve a number of problems in order to demonstrate how the formulas and graphs of the preceding sections can be used.

Example 1.- A wide-seal uniform-wall constant-thickness-lid Kovar package of the type shown in Figure 1 has the following dimensions (in inches);

$$a=b=.92 \qquad t=t_e=.015 \qquad h=.125 \qquad w=.040$$

and the following material properties:

$$E = E_w = 20\times10^6 \text{ psi} \qquad \nu = \nu_w = .3 \qquad \sigma_y = 50 \text{ ksi} \qquad \sigma_b = 107 \text{ ksi}$$

We wish to find the maximum tensile stress S_{max} in the seal and the central deflection δ_{max} of the lid due to an external screening pressure p of 30 psi; also the pressure $p_{ultimate}$ required to collapse the lid.

We first determine all the constants that will be needed to solve this problem. In accordance with Equation (7a) we take α to be 2, after which Equation (8b) and Figure 5 give

$$K = \frac{4}{\pi^2}\,\frac{.92}{.125}\left(\frac{.040}{.015}\right)^3 2 = 113 \qquad \arctan K = 1.56$$

(The closeness of arctan K to $\pi/2$ indicates that in effect the walls are clamping the edges of the lid.) Entering Figures 7, 8, 13, 14, 17 and 18 with b/a = 1 and arctan K = 1.56, we obtain

$$n_1 = .051 \quad n_2 = .443 \quad n_8 = 10.7 \quad n_4 = .00125$$

$$n_4(0) = .00406 \quad n_9 = .0737$$

Also, for p = 30 psi, we have

$$\frac{pa^4}{Et^4} = \frac{30}{20\times10^6}\left(\frac{.92}{.015}\right)^4 = 21.1$$

Since the wall cross-sectional area (wh) is only around one-third of the lid cross-sectional area (ta) and arctan K is very close to $\pi/2$, we shall use part (c) of Figure 15 to find

$$n_5 = .981$$

Equation (13a) gives

$$n = 6(.051) + 2(.443)\left(\frac{.04}{.92}\right) - \left(\frac{.04}{.92}\right)^2 = .343$$

Finally, from Equation (2),

$$m = m_e = (107{,}000)(.015)^2/6 = 4.0125 \text{ in.-lb/in.}$$

whence (Eq. (15))

$$p_t = \frac{m_e}{n_1 a^2} = \frac{4.0125}{(.051)(.92)^2} = 93 \text{ psi}$$

and the right sides of Equations (35) and (38) are, respectively,

$$\delta_{max_1} = 10.92\left(\frac{30}{20\times10^6}\right)\left(\frac{.92}{.015}\right)^3 (.92)(.00125)(.981) = .0043 \text{ in.}$$

$$\delta_{max_2} = \frac{(10.92)(.92)^2}{(20\times10^6)(.015)^3}\,[30(.92)^2(.00406) - (4.0125)(.0737)]$$

$$= .1369\ [.1031 - .2957] = -.026 \text{ in.}$$

We now have all the constants needed to determine the quantities we are looking for. We start with S_{max}. Since Kovar is ductile and the screening pressure p(= 30 psi) is less than the transition pressure p_t (= 93 psi), the upper left hand box of Table 1 applies. It gives

$$S_{max} = 30\left(\frac{.92}{.04}\right)^2(.343) = 5443 \text{ psi}$$

as the maximum tensile stress in the seal. This would be a safe stress if the solder were one of the higher strength types, such as a gold-tin alloy but it would be only marginally safe if the solder were a lead-tin alloy.

To determine the central deflection of the lid we make use of rule (39) which states that δ_{max} is the larger of δ_{max_1} and δ_{max_2}. Thus

$$\delta_{max} = \delta_{max_1} = .0043 \text{ in.}$$

This is 29% of the lid thickness but only 3% of the cavity depth. The fact that δ_{max_1} governed indicates that the lid is still in the linearly elastic region OA of the simplified pressure-deflection curve of Figure 16.

The collapse pressure is given by Equation (31) as

$$P_{ultimate} = (10.7)\,\frac{2(4.0125 + 4.0125)}{(.92)^2} = 203 \text{ psi}$$

which is well above the screening pressure of 30 psi.

Example 2.- Suppose that 30 psi is considered a satisfactory screening pressure for the package of Example 1 (to be referred to as package I).

What screening pressure would be appropriate for a second package (package II) identical in all respects to package I except for the dimension b, which has been increased to 1.92 in.?

For package II we still have arctan K = 1.56, but

$$\frac{b}{a} = \frac{1.92}{.92} = 2.1 \qquad \frac{a}{b} = .48$$

Figures 7 and 8 now give

$$n_1 = .083 \qquad n_2 = .513$$

and from Equation (13a) we obtain the following value of n for package II:

$$n = 6(.083) + 2(.513)\left(\frac{.04}{.92}\right) - \left(\frac{.04}{.92}\right)^2 = .541$$

Then, from Equation (16),

$$S_{max_t} = \frac{(4.0125)(.541)}{(.083)(.040)^2} = 16{,}346 \text{ psi}$$

In accordance with the discussion preceding Equation (25), a suitable screening pressure for package II is one that will produce the same S_{max} in its seal as 30 psi produced in the seal of package I, namely 5443 psi. Thus, in the formulas of Table 2 we may take S_{accept} to be 5443 psi. Since this is smaller than S_{max_t}, the leftmost formula of Table 2 applies. It gives the following appropriate screening pressure for package II:

$$p = \frac{5443}{\left(\frac{.92}{.04}\right)^2 (.541)} = 19 \text{ psi}$$

Example 3.- Let us repeat Example 1, assuming now that the seal is a solderless electrically welded seal of the narrow type (Figure 3(b) with

w_s = .010 in., and that the edge of the lid is thinned to a thickness of t_e = .004 in. while the main thickness t remains .015 in.

The calculations of Example 1 up to, but not including, the evaluation of n are valid here. Since the seal is now of the narrow type, Equation (13b) must be used for determining n. With w_s = .010 in., we have e = .035 in., and Equation (13b) then gives

$$n = [.051 - \frac{1}{2}(\frac{.04}{.92})^2]\frac{(.04)^2}{(.035)(.010)} = .229$$

Furthermore, while the fully plastic bending strength m in the main part of the lid remains 4.0125 in.-lb/in., in the thinned edge it goes down to

$$m_e = (107{,}000)(.004)^2/6 = 0.2853 \text{ in.-lb/in.}$$

according to Equations (2), whence

$$p_t = \frac{m_e}{n_1 a^2} = \frac{0.2853}{(.051)(.92)^2} = 6.6 \text{ psi}$$

The right side of Equation (33) remains at the value δ_{max_1} = .0043 in., but the new m_e value changes the right side of Equation (38), so that now

$$\delta_{max_2} = \frac{(10.92)(.92)^2}{(20\times10^6)(.015)^3}[30(.92)^2(.00406)-(.2853)(.0737)] = .0112 \text{ in.}$$

Proceeding as in Example 1, we note that the screening pressure p (= 30 psi) is now greater than p_t (= 6.6 psi) and that the seal is now a narrow one. Therefore the bottom right box of Table 1 applies, giving

$$S_{max} = \frac{.2853}{(.01)(.035)}[1 - \frac{1}{2(.051)}(\frac{.04}{.92})^2] = 800 \text{ psi}$$

as the maximum seal stress produced in the course of applying p. Since the seal material in this case is Kovar with an ultimate tensile strength on the order of 75,000 psi, the 800 psi maximum seal stress can be considered harmless to the integrity of the seal. From the absence of p in the formula for S_{max}, it can also be concluded that S_{max} would be the same for all screening pressures greater than the transition pressure p_t = 6.6 psi. The effect of using screening pressures greater than 6.6 psi is simply to spread the length of seal periphery over which the S_{max} of 800 psi is developed.

Turning to the deflections and again using rule (39), we obtain

$$\delta_{max} = \delta_{max_2} = .0112 \text{ in.}$$

This is 2.6 times larger than the δ_{max} produced by the same screening pressure in the lid of Example 1, but still only a small percentage (9%) of the total cavity depth.

Finally, from Equation (31) we estimate the collapse pressure to be

$$p_{ultimate} = (10.7)\frac{2(.2853 + 4.0125)}{(.92)^2} = 109 \text{ psi}$$

which is approximately half that of the lid of Example 1.

The present example serves to show that a thinned edge and lid plasticity can combine to provide a barrier against severe stressing of the seal under external pressure, but at the same time tend to increase the lid central deflection and reduce the lid collapsing pressure.

Example 4.- Assume that the package of Example 1 has its base changed from Kovar to ceramic with a thickness of .025 in., a modulus of elasticity of 50×10^6 psi, and a flexural strength of 65 ksi. What external pressure $p_{ultimate}$ will cause the base to crack?

We shall imagine the package turned upside down, so that the base becomes in effect a lid with

$$t = .025 \text{ in.} \qquad E = 50\times10^6 \text{ psi} \qquad \sigma_b = 65 \text{ ksi}$$

and, in accordance with the discussion in Section VII. A , we shall make two estimates of $p_{ultimate}$, one based on Equation (28), the other on Equation (30), and select the smaller of the two.

We start with Equation (28), which gives

$$n_7 = \frac{65\times10^3}{50\times10^6}\left(\frac{.92}{.025}\right)^2 = 1.76$$

as the values of n_7 required to cause fracture. The extensional stiffness Eat of the ceramic base is much higher than the corresponding stiffness $E_w hw$ of the wall. Therefore parts (a) and (c) of Figure 12 are the ones that apply. Assuming that the walls essentially clamp the edges of the base* (as they do the lid), we narrow the choice further to part (c) alone. It gives the following as the value of pa^4/Et^4 needed to achieve an n_7 of 1.76 with a b/a of 1.0:

$$\frac{pa^4}{Et^4} = 5.6$$

whence the pressure required to crack the base is

$$p_{ultimate_1} = \frac{5.6\ Et^4}{a^4} = \frac{(5.6)(50\times10^6)(.025)^4}{(.92)^4} = 153 \text{ psi}$$

Proceeding now on the basis of Equation (30), we first compute (Eq. (8b))

---

*This assumption will be justified presently when arctan K is computed and found to be quite close to $\pi/2$.

$$K = \frac{4}{\pi^2}\frac{.92}{.125}\frac{50}{20}\left(\frac{.040}{.015}\right)^2 2 = 61 \qquad \arctan K = 1.554$$

Then from Figure 7, $n_1 = .05$. Therefore Equation (30) gives

$$P_{ultimate_2} = \frac{65{,}000}{6(.05)}\left(\frac{.025}{.92}\right)^2 = 160 \text{ psi}$$

as the second estimate. This is slightly higher than the previous estimate and is therefore not the governing one. We are left with

$$P_{ultimate} = P_{ultimate_1} = 153 \text{ psi}$$

as the best estimate of the pressure required to fracture the ceramic base.

Example 5.- Suppose the package of Example 4 to be placed in a centrifuge in such a way that the centrifugal force tends to push the ceramic base into the cavity. Taking the specific gravity of the ceramic to be 3.85, determine how many g's of centrifuge acceleration are required to crack the base.

We first convert the specific gravity of 3.85 to a specific weight, d, by multiplying it by the specific weight of water, which is .0361 lbs/in.^{3}. The result is

$$d = .139 \text{ lbs/in.}^3$$

The pressure required to crack the base is 153 psi, from Example 4. The equivalence relation (41) therefore gives

$$G = \frac{153 \text{ lb/in.}^2}{(.025 \text{ in.})(.139 \text{ lb/in.}^3)} = 44{,}000 \text{ g's}$$

of centrifuge acceleration required to crack the base. In this calculation, since the base is already close to being clamped at its edges, we have ignored the fact that of α may be different (higher) for centrifuge loading than for external pressure (see the discussion of this point in Section IX).

Example 6.- A stepped-wall wide-seal package with a constant-thickness Kovar lid has the following dimensions (in inches):

$a = .365$	$b = .670$	$t = t_e = .025$
$h = .082$	$h_1 = .060$	$h_2 = .025$
$w = .040$	$w_1 = .049$	$w_2 = .071$

and the following mechanical properties:

$E = E_w = 20\times10^6$ psi (Kovar) $\quad E_1 = E_2 = 8.6\times10^6$ psi (glass)

$\nu = \nu_w = 0.3 \quad\quad \nu_1 = \nu_2 = 0.2$

$\sigma_b = 107{,}000$ psi for the Kovar lid

Determine the maximum tensile stress S_{max} produced in the seal by a screening pressure p of 100 psi.

From Equations (1) and (4) we have

$$D = \frac{(20\times10^6)(.025)^3}{12(.91)} = 28.6 \text{ in-lb}$$

$$D_w = \frac{(20\times10^6)(.040)^3}{12(.91)} = 117.5 \text{ in-lb}$$

$$D_1 = \frac{(8.6\times10^6)(.049)^3}{12(.96)} = 87.9 \text{ in-lb}$$

$$D_2 = \frac{(8.6\times10^6)(.071)^3}{12(.96)} = 267 \text{ in-lb}$$

Then Equation (7b) gives

$$\alpha = \frac{2}{1 - \left(\frac{h_1}{h}\right)^2 + \frac{D_w}{D_1}\left[\left(\frac{h_1}{h}\right)^2 - \left(\frac{h_2}{h}\right)^2\right] + \frac{D_w}{D_2}\left(\frac{h_2}{h}\right)^2}$$

$$= \frac{2}{1 - \left(\frac{.060}{.082}\right)^2 + \frac{117.5}{87.9}\left[\left(\frac{.060}{.082}\right)^2 - \left(\frac{.025}{.082}\right)^2\right] + \frac{117.5}{267}\left(\frac{.025}{.082}\right)^2}$$

$$= 1.82$$

whence (Equation (8) and Figure 5)

$$K = \frac{4}{\pi^2}\ \frac{.365}{.082}\ \frac{117.5}{28.6}\ (1.82) = 11.1 \qquad \text{and arctan } K = 1.48$$

From the given dimensions we have

$$\frac{a}{b} = \frac{.365}{.670} = .545 \qquad \frac{b}{a} = 1.83$$

Entering these values, together with arctan K = 1.48, into Figures 7 and 8, we find

$$n_1 = .074 \qquad n_2 = .515$$

From Equation (2), $m = m_e = (107{,}000)(.025)^2/6 = 11.146$ psi, whence

$$p_t = \frac{m_e}{n_1 a^2} = \frac{11.146}{(.074)(.365)^2} = 1131 \text{ psi}$$

Since this is greater than the screening pressure of 100 psi, the upper left hand box of Table 1 applies, giving

$$n = 6(.074) + 2(.515)\left(\frac{.040}{.365}\right) - \left(\frac{.040}{.365}\right)^2 = .545$$

and

$$S_{max} = (100)\left(\frac{.365}{.040}\right)^2 (.545) = 4540 \text{ psi}$$

XI. EXPERIMENTAL CONFIRMATION

A. General Considerations.- The three hypotheses listed in Section IV form the basis of that portion of the present work dealing with hermeticity failure. The first hypothesis reduces the lid to a uniformly loaded elastic rectangular plate with edges elastically restrained against rotation. It, together with certain assumptions regarding the distribution of stress across the width of the seal, leads to Equation (12) as the relationship between the external pressure p and the maximum tensile stress S_{max} in the seal for ductile lids under pressures less than the transition pressure p_t. The second and third hypotheses imply that loss of hermeticity in such cases occurs when S_{max} reaches the ultimate tensile strength S_{ult} of the seal material. Taken together with Equation (12), they permit the following seal strength S_{ult} to be inferred from the critical pressure p_{cr} at which loss of hermeticity is first observed to occur, provided that p_{cr} is less than p_t:

$$S_{ult} = p_{cr}\left(\frac{a}{w}\right)^2 n$$

This can be rewritten as

$$p_{cr} = S_{ult}\left[\left(\frac{a}{w}\right)^2 n\right]^{-1} \qquad (50)$$

Thus, for ductile lids losing hermeticity at pressures p_{cr} that are less

than p_t, the present hypotheses lead to a straight-line relationship between p_{cr} and the package parameter $[(a/w)^2 n]^{-1}$, with the straight line passing through the origin and having a slope equal to the ultimate tensile strength S_{ult} of the seal material (see Figure 20).

The validity of Equation (50), and therefore of the hypotheses on which it is based, can be tested by means of a fairly simple experimental program. The program would require ductile-lidded flat-packs of various sizes and shapes, all carefully and uniformly sealed with the same material. With the aid of Equations (13) and (15) the values of $[(a/w)^2 n]^{-1}$ and p_t would be determined for each package. Each package would also be subjected to an external pressure that is increased in small steps. The package would be leak-tested after each step, and the pressure p_{cr} at which it first loses hermeticity would be noted. Thus, for each package whose p_{cr} turned out to be less than p_t, the p_{cr} could be plotted against $[(a/w)^2 n]^{-1}$. If the plotted points all fell on a single straight line through the origin, as in Figure 21(a), that would imply perfect validation of the theory (Equation (50)), and the slope of the line would give the effective ultimate tensile strength of the seal material.

Of course, such perfect agreement between theory and experiment is not to be expected, partly because of undoubted shortcomings in the theory and partly because of unavoidable variations in sealing quality among the packages. This variability in sealing quality produces, in effect, a spectrum of S_{ult} values instead of a single one and would cause the test data to fall in a wedge-shaped band, as in Figure 21(b), with the angle of the wedge depending on the range of effective S_{ult} values achieved in the seals. If the tests are performed using several groups of packages,

with the packages nominally identical within each group but differing from group to group, the test data should fall as shown in Figure 21(c), provided that the range of variation of seal strengths was the same from group to group. If the range of seal strengths differed from group to group (as it might if the groups were of different size), the tops and bottoms of the vertical bars in Figure 21(c) would not lie on perfect straight lines through the origin. In that case, however, the mean p_{cr} values of the various groups, being less sensitive to sample size than the range of p_{cr} values, should still lie reasonably close to a single straight line. When the sample sizes in the various groups are different, a reduced range of p_{cr} values, covering one standard deviation above and below the mean p_{cr} value, would be preferable to total range as a plotting parameter, because the standard deviation of the S_{ult} values within any group of packages should also be less sensitive to sample size than the range of S_{ult} values. A hypothetical plot of test data using such a reduced range is shown in Figure 21(d).

B. Test Program.- Data furnished to the author by a package manufacturer constitutes, in effect, a test program of the type described above. It involved 579 packages distributed among eighteen groups, with the packages nominally identical within each group. The packages had three-segment stepped-type walls, as in Figure 2(b). The top segment was a Kovar seal frame; the two lower segments were glass beads sandwiching a lead frame. The lids were Kovar and were sealed to the wall by means of a gold-tin solder preform.

Each group of packages was placed in a pressure bomb and subjected to external air pressure that was increased in small steps. Each new

pressure was held for approximately 10 minutes, after which the packages were tested for gross leaks by submerging them in a heated liquid and watching for bubbles emanating from the interior of the package. The leakers were removed from the group and the rest of the group was then subjected to the next higher pressure.

The test program details are summarized in Table 3. Table 3 starts by giving the group designations (A1, A2, B, C, etc.) and the number of packages in each group. Lines 3 through 16 of the table then give the dimensional and material characteristics of the packages. It will be noted that groups A1 and A2 are nominally identical, as are groups G1 and G2. Thus, the results obtained from these two pairs of groups can serve to give some indication as to the degree of inherent variability resulting from the manufacturing, assembly and testing procedures. Lines 17 through 27 represent stages in the calculations leading up to the value of the parameters $[(a/w)^2 n]^{-1}$ and p_t for each package group, assuming that $p_{cr} < p_t$, so that Equation (13a) may be used for n. Line 28 shows the pressure increment employed in the leak testing, and lines 29 to 33 give the main statistical information regarding the p_{cr} values obtained for each group of packages. The detailed failure data on which lines 29 to 33 are based are contained in Table 4. In Table 4, p represents the pressure in psi and N the number of packages losing hermeticity at that pressure. Entries for which N = 0 are not included in the table.

Lines 27 and 29 of Table 3 and the detailed p_{cr} data of Table 4, show that, except for the strongest seals of the group O packages, the p_{cr} values are all below the p_t values, thus justifying the above-mentioned use of Equation (13a) as a basis for evaluating n and also justifying the type of data analysis proposed in part A of this section.

Table 3.- Test Program Summary

1	Group Designation		A1	A2	B	C	D	E	F	G1	G2	H	I	J	K	L	M	N	O	P
2	No. of packages in group		43	43	59	37	17	32	26	37	18	65	53	38	25	16	16	18	19	17
3	Nominal dimensions (inches)	a	1.129		.337	.315	.850	.850	.850	.209		.209	.772	.774	.788	.545	.547	.650	.630	.365
4		b	1.129		.337	.315	.910	.910	.910	.332		.332	.828	.830	.844	.545	.547	.900	.630	.670
5		t, t_e	.030		.010	.010	.015	.015	.020	.010		.010	.030	.030	.030	.015	.015	.015	.015	.025
6		h	.139		.054	.048	.083	.117	.117	.050		.053	.090	.115	.079	.113	.063	.105	.108	.082
7		h_1	.109		.044	.038	.068	.087	.087	.042		.043	.065	.088	.059	.098	.048	.090	.093	.060
8		h_2	.062		.027	.018	.045	.060	.060	.020		.020	.039	.035	.040	.045	.024	.045	.045	.025
9		w	.0755		.023	.030	.045	.046	.046	.0255		.0255	.0515	.0515	.046	.040	.0365	.0515	.060	.040
10		w_1	.0825		.0285	.0365	.056	.056	.056	.0295		.0295	.059	.059	.0525	.052	.044	.0655	.069	.049
11		w_2	.1275		.0475	.0675	.088	.0905	.0905	.064		.0475	.092	.089	.0905	.082	.0715	.098	.110	.071
12	Material constants	E, E_w	20,000,000 psi																	
13		E_1, E_2	8,600,000 psi																	
14		ν, ν_w	0.3																	
15		ν_1, ν_2	0.2																	
16		σ_b	107,000 psi																	
17	Derived quantities	b/a	1		1	1	1.07	1.07	1.07	1.59		1.59	1.07	1.07	1.07	1	1	1.39	1	1.84
18		a/b	1		1	1	.93	.93	.93	.63		.63	.93	.93	.93	1	1	.72	1	.54
19		e (Eq. 7b)	1.58		2.13	1.88	2.21	2.16	2.16	1.69		1.65	1.82	1.58	1.96	2.09	1.86	2.02	1.61	1.82
20		K (Eq. 8a)	82.7		65.5	135	248	183	77.4	47.5		43.7	31.9	21.9	28.5	77.6	94.2	206	243	13.5
21		arctan K	1.556		1.555	1.563	1.567	1.565	1.558	1.550		1.548	1.539	1.525	1.536	1.558	1.560	1.566	1.567	1.497
22		n_1 (Fig. 7)	.050		.050	.0505	.0556	.0556	.0549	.0756		.0755	.0535	.0526	.0531	.0501	.0501	.0715	.0505	.0755
23		n_2 (Fig. 8)	.443		.443	.443	.462	.462	.462	.515		.515	.461	.461	.462	.443	.443	.508	.443	.516
24		n (Eq. 13a)	.355		.356	.378	.380	.381	.376	.564		.564	.378	.373	.369	.360	.355	.503	.378	.554
25		$[(a/w)^2 n]^{-1}$	.0126		.0131	.0240	.0074	.0077	.0078	.0264		.0264	.0118	.0119	.0092	.0149	.0125	.0125	.0240	.0217
26		m_e (lb)(Eq.2)	16.05		1.783		4.0125		7.133	1.783			16.05			4.0125				11.146
27		p_r (psi)(Eq.15)	252		314	356	100		180	540		541	503	509	487	270	268	133	200	1108
28	Pressure increment (psi)		5	5	10	10	5	5	5	10	10	10	10	10	5	10	5	5	10	10
29	P_{cr} data (psi)	maximum	110	110	180	250	55	55	50	400	300	240	140	150	90	180	115	120	220	390
30		minimum	70	75	90	160	25	45	35	140	190	140	90	90	75	80	70	70	140	300
31		median	90	110	140	190	45	50	42.5	270	240	200	120	120	85	120	105	100	190	360
32		mean	92	97	139	202	43	51	43	273	247	192	121	123	84	124	92	98	183	353
33		std. dev.	9.6	8.3	17.8	27.3	7.3	3.1	4.3	54.8	32.0	25.3	13.3	13.3	3.9	25.8	17.7	14.6	24.7	27.6

Table 4.- Leak Test Failure Data

A1		A2		B		C		D		E		F		G1		G2		H		I		J		K		L		M		N		O		P	
p	N	p	N	p	N	p	N	p	N	p	N	p	N	p	N	p	N	p	N	p	N	p	N	p	N	p	N	p	N	p	N	p	N	p	N
70	1	75	2	90	1	160	1	25	1	45	3	35	2	140	1	190	1	140	3	90	1	90	1	75	1	80	1	70	4	70	1	140	2	300	1
75	1	80	1	110	4	170	8	35	1	50	18	40	11	150	1	200	1	150	7	100	6	100	1	80	8	90	1	75	2	75	2	150	1	310	1
80	5	85	3	120	9	180	4	40	2	55	11	45	9	160	1	210	1	160	2	110	9	110	3	85	12	100	1	80	1	85	1	160	1	320	1
85	7	90	3	130	7	190	7	45	7			50	4	230	3	220	1	170	2	120	16	120	18	90	4	110	2	105	7	90	1	170	4	330	2
90	10	95	10	140	20	200	1	50	4					240	4	230	2	180	3	130	11	130	10			120	4	110	1	95	3	180	1	340	2
95	7	100	13	150	10	220	3	55	2					250	4	240	5	190	9	140	10	140	4			130	3	115	1	100	2	190	3	360	2
100	5	105	9	160	3	230	10							260	3	260	2	200	18			150	1			140	2			105	5	200	2	370	5
105	4	110	2	170	3	240	2							270	2	280	2	210	11							170	1			115	1	210	4	380	1
110	3			180	2	250	1							280	1	290	2	220	4							180	1			120	2	220	1	390	2
														290	5	300	1	230	4																
														300	2			240	4																
														310	2																				
														320	4																				
														330	1																				
														340	1																				
														380	1																				
														400	1																				

C. Results.- Line 25 of Table 3 furnishes abscissa values for the types of plots discussed in part A; ordinate values are obtained from one or more of the last five lines of Table 3.

The most significant representation of the results is that given in Figure 22, where the mean p_{cr} values are plotted as a function of $[(a/w)^2 n]^{-1}$. Except for group P the mean p_{cr} values fall reasonably close to a line emanating from the origin, as predicted by the theory. The solid straight line is the best fit, in least-squares sense, to all the plotted points, excluding group P. Its slope leads to an inferred ultimate tensile strength of 8450 psi, which is considered quite reasonable for the glass beneath the seal frame.* Although there is some scatter of the test data relative to the straight line, it is not considered excessive in view of the inherent variability, as evidenced by the different mean p_{cr} values for the nominally identical packages G1 and G2.

The dashed straight lines in Figure 22 correspond to other inferred values for the tensile strength of the seal. It is seen that the stronger packages have an inferred seal strength of approximately 10,200 psi, which is one of the higher values quoted to the author for the tensile strength of the glass. The lowest dashed line shows that all of the packages achieved a mean inferred seal strength of 5000 psi or more. Packages P turned out to be considerably stronger in terms of their mean p_{cr} value, than the theory would indicate. There is no explanation for this discrepancy, although it may be significant that these packages are the most oblong, with a b/a ratio

*The quoted strength of the gold-tin solder at the top of the seal frame is 18,900 psi. Therefore the glass, with quoted strengths of 10,200 psi and less, is considered to be the weak link in these packages.

of 1.84. It is also interesting that the inferred seal strength for the P packages is 16,300 psi, which is not far from the 18,900 psi value quoted for the gold-tin solder preform. This agreement is undoubtedly coincidental, since in the leak testing the bubbles were observed to come from between the seal frame and the glass, not from between the seal frame and the lid.

In Figure 23, the test results are plotted in such a way as to show the range of p_{cr} values from one standard deviation above the mean to one standard deviation below the mean. The fact that the heights of the bars tend to increase as the abscissa increases is considered a partial validation of the theory, since the theory predicts that a given range of seal strengths will lead to a range of p_{cr} proportional to $[(a/w)^2 n]^{-1}$ (see Equation (50)).

In Figure 24, the entire experimental range of p_{cr} values is plotted for each package. The heights of some of the vertical bars (e.g., in the case of the G1 packages) emphasize once again the degree of variability inherent in the p_{cr} values of nominally identical packages and tend to support the author's earlier assertion that the scatter shown in Figure 22 is not excessive. The dashed lines in Figure 24 show that none of the individual packages had an inferred seal strength less than 3220 psi or greater than 18,000 psi.

In general the experimental results tend to confirm the theoretical hypotheses related to loss of hermeticity.

XII. CONCLUSIONS

Simple formulas have been presented that are related to the mechanical behavior of microelectronic flat-packs under external pressure and can

assist in the design of such packages or the selection of suitable screening pressures for testing their hermeticity.

The specific items covered by the formulas are: maximum tensile stress in the lid-to-wall seal (or seal-frame-to-glass-bead seal), central deflection of the lid, pressure required to crack or collapse the lid, and the equivalence of external pressure and centrifuge acceleration insofar as lid behavior and seal stresses are concerned.

Numerical examples have been presented to illustrate the use of the formulas, and experimental data have been presented which tend to confirm some of the formulas and hypotheses related to loss of hermeticity under external pressure.

From the numerical examples as well as the calculations related to the test specimens it appears that in many cases a simplifying assumption would be justifiable, namely the assumption that the edges of the lid are fully clamped by the walls to which they are joined. This permits one to set the elastic restraint parameter K equal to infinity (arctan K = $\pi/2$), and thus avoid the sometimes tedious precise evaluation of this parameter.

APPENDIX A: SYMBOLS

a	width of lid as measured inside the cavity, in. ($a \leq b$)
b	length of lid as measured inside the cavity, in. ($b \geq a$)
d	specific weight of lid material, lb/in^3
D	plate flexural stiffness of lid, defined by Equation (1), in-lb
D_w	plate flexural stiffness of wall or of top segment of step-type wall, defined by Equation (3), in-lb
D_1	plate flexural stiffness of second segment of step-type wall, defined by Equation (4), in-lb
D_2	plate flexural stiffness of third segment of step-type wall, defined by Equation (4), in-lb
e	distance from inner edge of wall top to middle of width of narrow seal, in. (Fig. 3(b))
E	Young's modulus of lid material, psi
E_w	Young's modulus of wall or of top segment of step-type wall, psi (Fig. 2(b))
E_1	Young's modulus of second segment of step-type wall, psi (Fig. 2(b))
E_2	Young's modulus of third segment of step-type wall, psi (Fig. 2(b)
g	acceleration of gravity, 32.2 ft/sec^2, 386 in./sec^2
G	centripetal acceleration in units of g, dimensionless
$G_{equivalent}$	centripetal acceleration, in g's, equivalent to a given pressure, defined by Equation (41), dimensionless
h	height of wall, measured inside cavity, in. (Fig. 2)
h_1	height to top of second segment of step-type wall, in. (Fig. 2(b))
h_2	height to top of third segment of step-type wall, in. (Fig. 2(b))

k	wall rotational stiffness defined by Equation (5) and evaluated by Equations (7), in-lb/in.
K	dimensionless wall stiffness defined by Equations (8)
m, m_e	fully plastic bending moments of lid, evaluated by Equations (2), in-lb/in.
M	local bending moment per unit width at top of wall, in-lb/in.
M_{max}	maximum value of M, occurring at middle of long side, in-lb/in.
M_b	local bending moment per unit width at bottom of wall, in-lb/in.
n	number of segments in step-type wall, dimensionless; also dimensionless constant defined by Equation (12) and evaluated by Equations (13)
n_1	dimensionless constant defined by Equation (9) and evaluated by Figure 7
n_2	dimensionless constant defined by Equation (10) and evaluated by Figure 8
n_4	dimensionless constant defined by Equations (33) and (34) and evaluated by Figure 14
$n_4(0)$	value of n_4 for K = 0; plotted in Figure 17
n_5	large-deflection theory correction factor to n_4, defined by Equation (35) and evaluated by Figure 15, dimensionless
n_7	dimensionless constant defined by Equation (27) and evaluated by Figure 12
n_8	dimensionless constant defined by Equation (31) and evaluated by Equation (32) or Figure 13
n_9	dimensionless constant defined by Equation (37) and plotted in Figure 18

N	number of packages losing hermeticity at a given screening pressure, dimensionless
p	net pressure acting inward on lid, psi
p_{cr}	pressure causing loss of hermeticity, psi
p_I	screening pressure for a previous package, psi
p_{II}	screening pressure for a new package, psi
$p_{equivalent}$	effective pressure due to a centrifuge acceleration, defined by Equation (40), psi
p_t	"transition pressure" defined by Equation (15)
$p_{ultimate}$	collapsing pressure for lid, psi
$p_{ultimate_1}$	collapsing pressure defined by Equation (28)
$p_{ultimate_2}$	collapsing pressure defined by Equation (30)
S_{accept}	*minimum* acceptable strength of seal material, psi
S_{all}	allowable tensile stress in seal, psi
S_{max}	maximum tensile stress in seal, psi
S_{max_t}	"transition" seal stress defined by Equation (16)
t	main thickness of lid, in.
t_e	edge thickness of lid, in.
V	effective vertical shear intensity at edge of lid, lb/in.
V_{max}	maximum value of V, occurring at middle of long side, lb/in.
w	thickness of wall or of top segment of wall, in. (Fig. 2)
w_1	thickness of second segment of step-type wall, in. (Fig. 2(b))
w_2	thickness of third segment of step-type wall, in. (Fig. 2(b))
w_s	width of seal, in. (Fig. 3)

GREEK:

α	dimensionless proportionality constant defined by Equation (6) and evaluated by Equations (7), (47) or (48)
β	constant defined by Equation (46) and evaluated by Equations (46) or (49)
δ_{max}	central deflection of lid, in.
δ_{max_1}	central deflection defined by Equations (33) and (34)
σ_{max_2}	central deflection defined by Equation (38)
θ	local angle of rotation of top of wall, radians
μ	parameter defined in Figure 25, dimensionless
ν	Poisson's ratio of lid material, dimensionless
ν_w	Poisson's ratio of wall or of top segment of step-type wall, dimensionless (Fig. 2(b))
ν_1, ν_2	Poisson's ratios of second and third segments, respectively, of step-type wall, dimensionless (Fig. 2(b))
σ_b	flexural strength (bending modulus of rupture) of lid material, psi
σ_{max}	maximum tensile stress in lid, psi
σ_t	ultimate tensile strength of lid material, psi

SUBSCRIPTS:

I	previous package
II	present package

APPENDIX B:

ORIGIN OF COLLAPSING PRESSURE FORMULA, EQUATION (31), FOR DUCTILE-MATERIAL LIDS

The uniform lateral pressure required to collapse a plate of ductile material can be estimated by means of a "yield-line analysis" similar to the limit analysis technique used for rigid-jointed frames. The yield-line analysis method is explained in Reference 9.

Applying this method to the rectangular lid of a flat pack, with an assumed yield-line pattern as represented by the dashed lines in Figure 25, and with μ therein so chosen as to minimize the collapse load, one easily arrives at the following formula for the collapsing pressure, $p_{ultimate}$, for the case $a/b \leq 1$:

$$p_{ultimate} = \frac{48}{[\sqrt{3 + (a/b)^2} - (a/b)]^2} \frac{m_e + m}{2a^2} \qquad (B1)$$

The yield-line pattern of Figure 21 is a plausible one for the limiting case $a/b \to 0$. However, at the other limit, $a/b = 1$, E.N. Fox (Reference 10) has found for a constant thickness lid that a more sophisticated yield line arrangement prevails which leads to a factor 42.8 in place of the factor 48 in Equation (B1). Therefore we shall multiply the right side of (B1) by the correction factor

$$\frac{48 - 5.2(a/b)}{48} \qquad (B2)$$

which has no effect when $a/b = 0$, but reduces the 48 to 42.8 when $a/b = 1$ and for simplicity varies linearly in a/b.

Equation (B1) then becomes

$$p_{ultimate} = n_8 \cdot \frac{2(m_e + m)}{a^2} \tag{B3}$$

where

$$n_8 = \frac{12 - (1.3)(a/b)}{\left[\sqrt{3 + (a/b)^2} - (a/b)\right]^2} \tag{B4}$$

This equation is plotted in Figure 25. It is found that the resulting graph can be represented very well by the following second-degree parabola:

$$n_8 = 4 + 3.2\,\frac{a}{b} + 3.5\,\left(\frac{a}{b}\right)^2 \tag{B5}$$

This is the representation used in Equation (32).

REFERENCES

1. "Test Methods and Procedures for Microelectronics." MIL-STD-883-B, Rome Air Development Center (AFSC), Griffiss Air Force Base, New York, 31 August 1977.

2a. Libove, C.: "Rectangular Flat-Pack Lids under External Pressure." RADC-TR-76-118, May 1976. (DDC No.: AD-A025625).

2b. Libove, C.: "Rectangular Flat-Pack Lids under External Pressure: Formulas for Screening and Design." 13th Annual Proceedings/ Reliability Physics 1975, Las Vegas, Nevada, April 1-3, 1975, pp. 38-47. Publication No. 75CH0931-6 PHY, Institute of Electrical and Electronic Engineers, 345 East 47th Street, New York, New York 10017.

3. Libove, C.: "Rectangular Flat-Pack Lids Under External Pressure: Improved Formulas for Screening and Design." RADC-TR-76-291, September 1976. (DDC No.: AD-A032490).

4. Timoshenko, S.; and Woinowski-Krieger, S.: "Theory of Plates and Shells." McGraw-Hill Book Company, Inc., New York, 1959.

5. Kornishin, M.S.; and Isanbayeva, F.S.: "Flexible Plates and Panels." Report FTD-HC-23-441-69, Air Force Systems Command, Foreign Technology Division, January 21, 1971, AD 722 302. (Translation of Russian book Gibkiye Plastiny i Paneil, 1968).

6. Aalami, B.; and Williams, D.G.: "Thin Plate Design for Transverse Loading." John Wiley & Sons, New York, 1975.

7. Lin, T.H.; Lin, S.R.; and Mazelsky, B.: "Elastoplastic Bending of Rectangular Plates," Journal of Applied Mechanics, December 1972, pp. 978-982.

8. "Properties of AlSiMag Brand Ceramics." Bulletin No. 757, Technical Ceramic Products Division, 3M Company, St. Paul, Minnesota.

9. Jones, L.L.; and Wood, R.H.: "Yield-Line Analysis of Slabs." American Elsevier Publishing Co., Inc., New York, 1967.

10. Fox, E.N.: "Limit analysis for plates: the exact solution for a clamped square plate of isotropic homogeneous material obeying the square yield criterion and loaded by uniform pressure." Philosophical Transactions of the Royal Society of London; A. Mathematical and Physical Sciences, vol. 22, no. 1265, pp. 121-155, 29 August 1974.

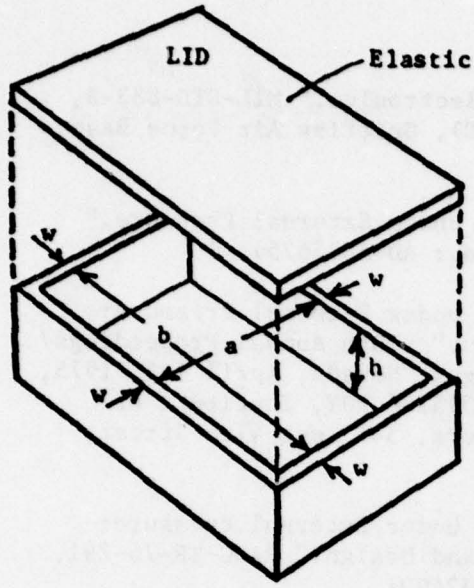

Figure 1.- Package configuration.

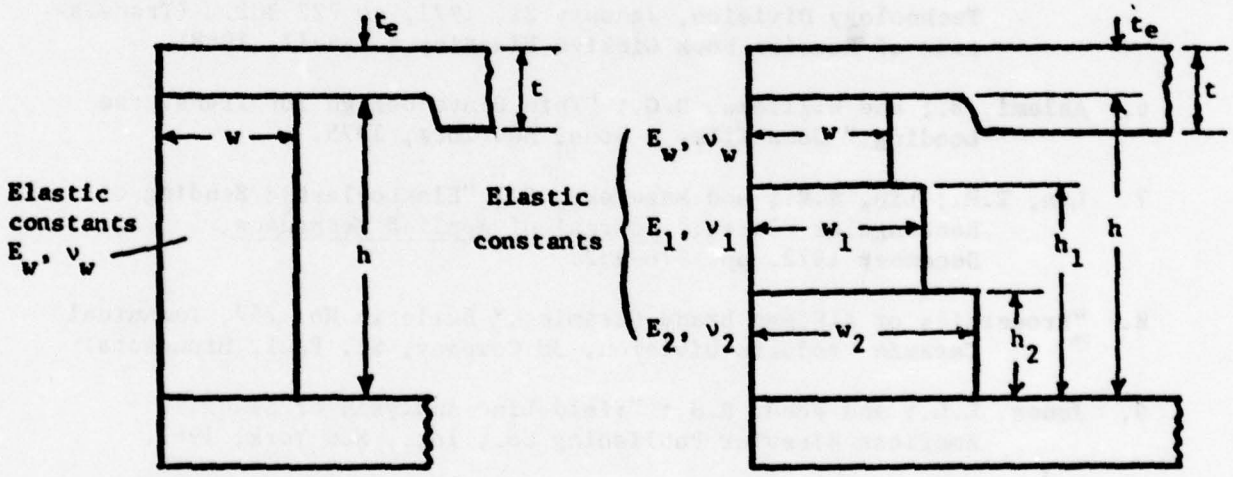

(a) Uniform wall

(b) Stepped wall

Figure 2.- Wall configurations.

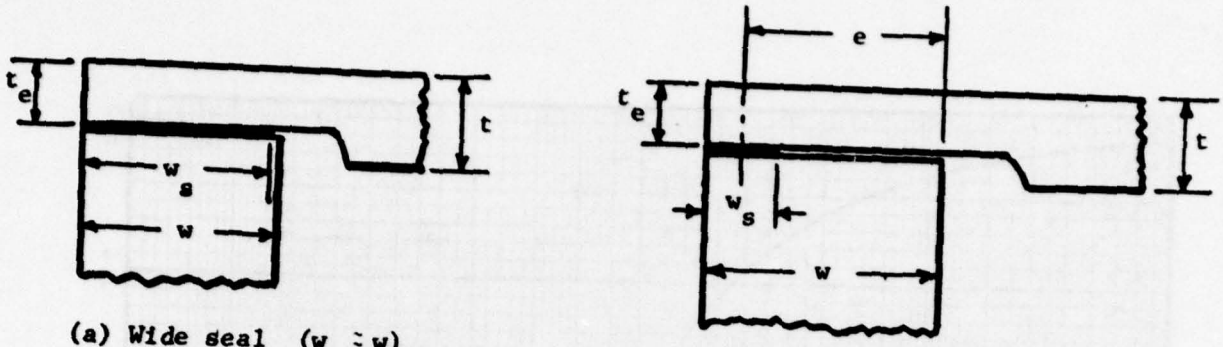

(a) Wide seal ($w_s \simeq w$)

(b) Narrow seal ($w_s << w$)

Figure 3.- Lid-to-wall seal geometries.

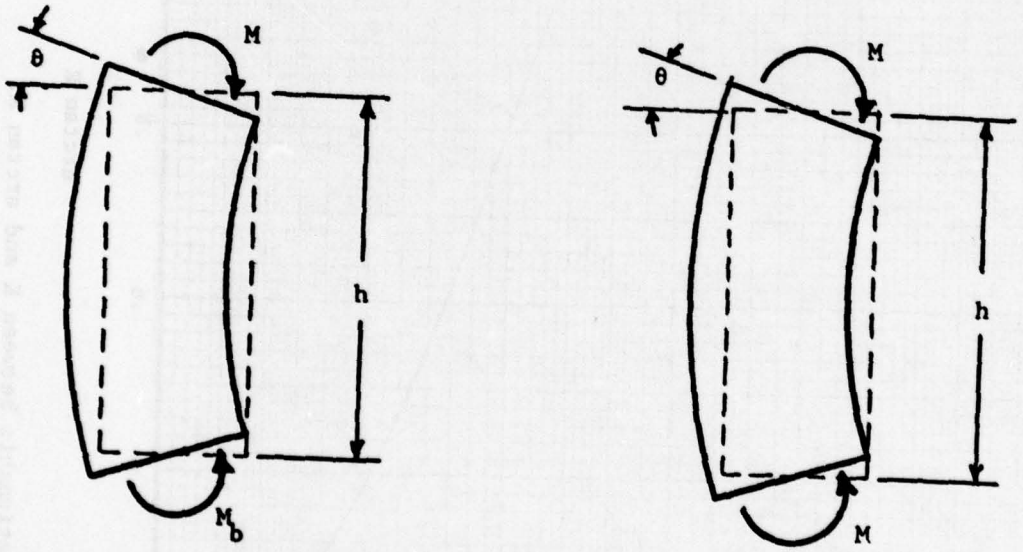

(a) Unequal moments at top and bottom of wall.

(b) Equal moments at top and bottom of wall.

Figure 4.- Wall flexure due to bending moments applied at top and bottom by lid and base.

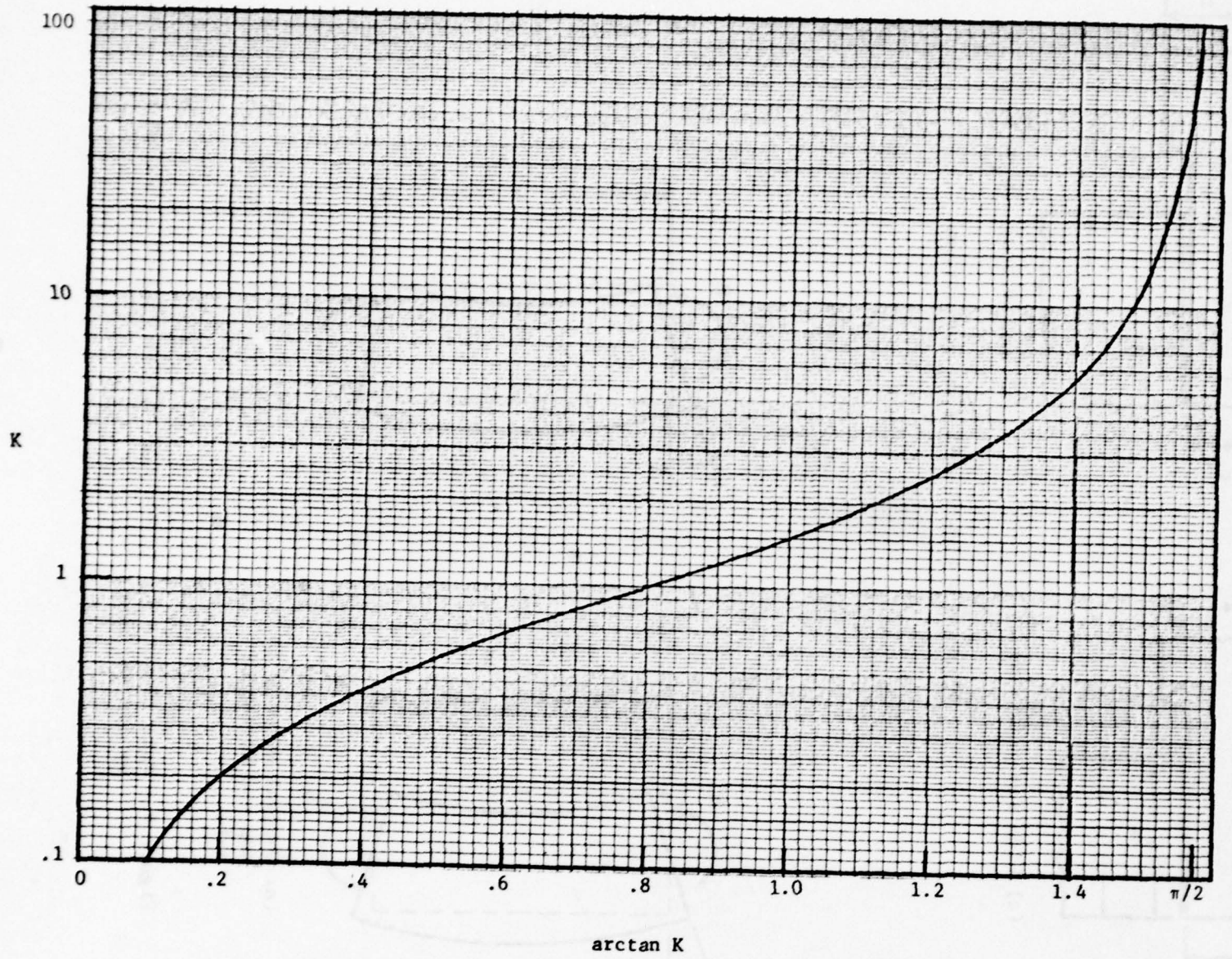

Figure 5.- Relationship between K and arctan K.

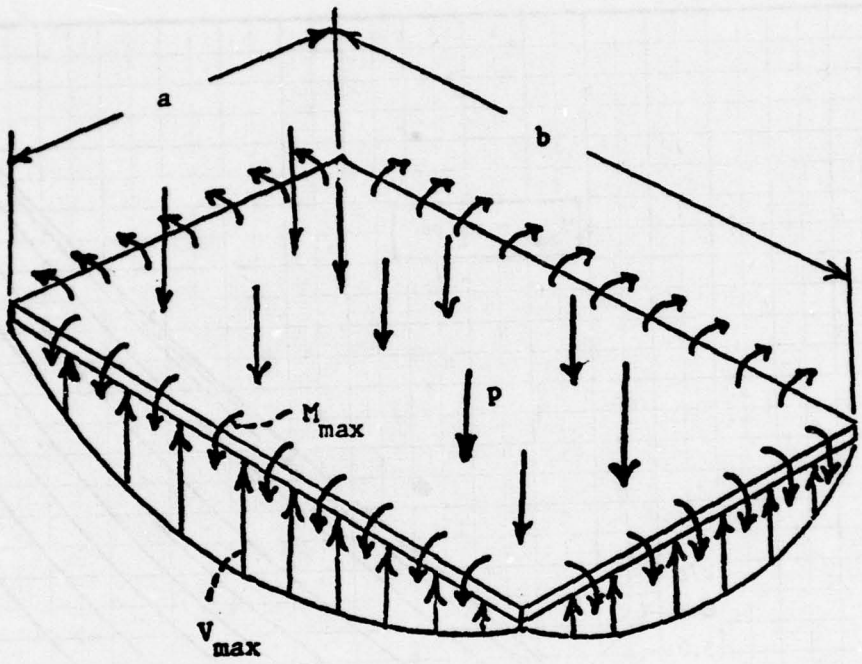

Figure 6.- Reactions on a uniformly loaded rectangular plate with edges elastically restrained against rotation.

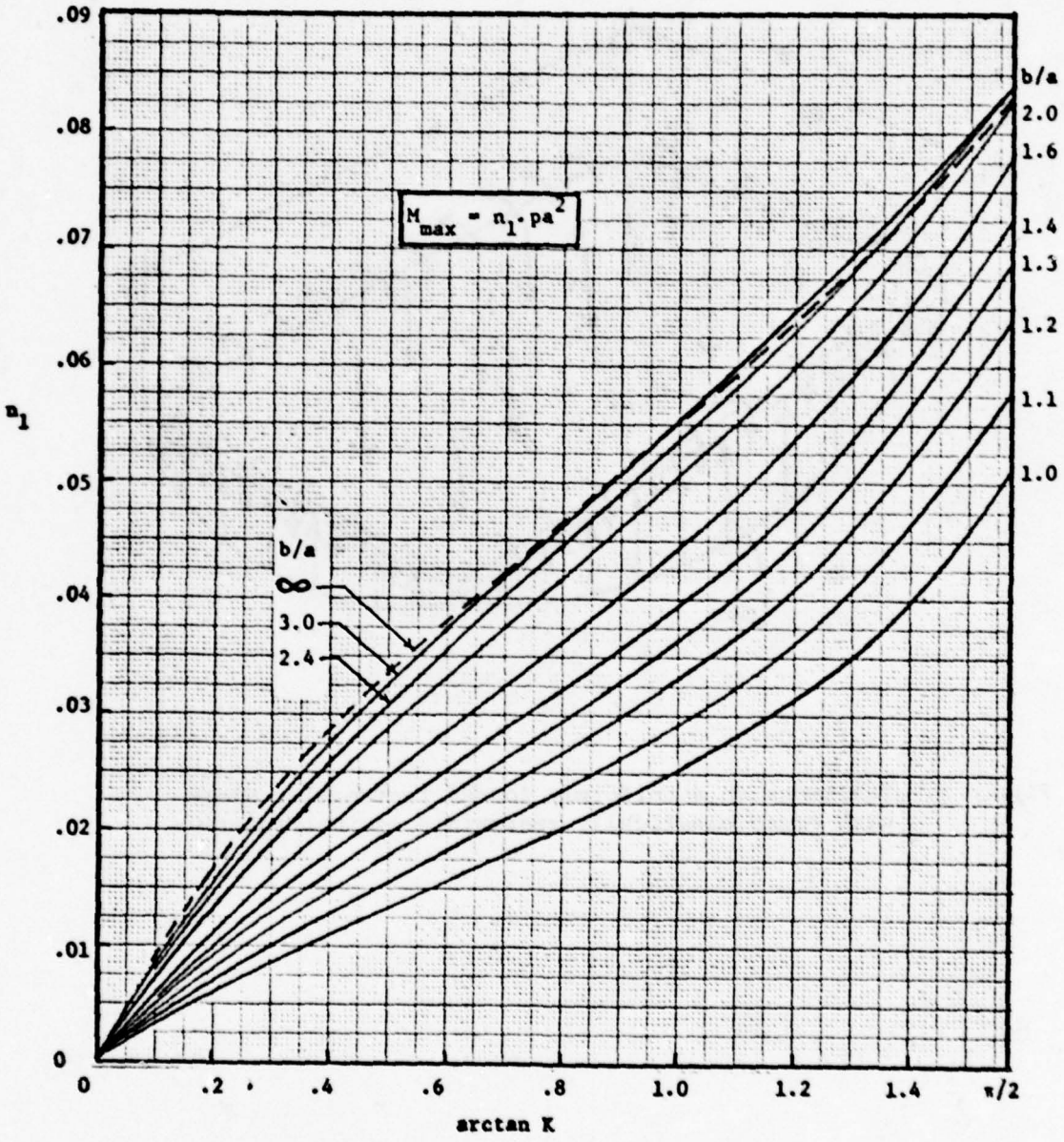

Figure 7.- Bending moment intensity at the middle of the long side for a uniformly loaded rectangular plate obeying Hooke's law with edges elastically restrained against rotation.

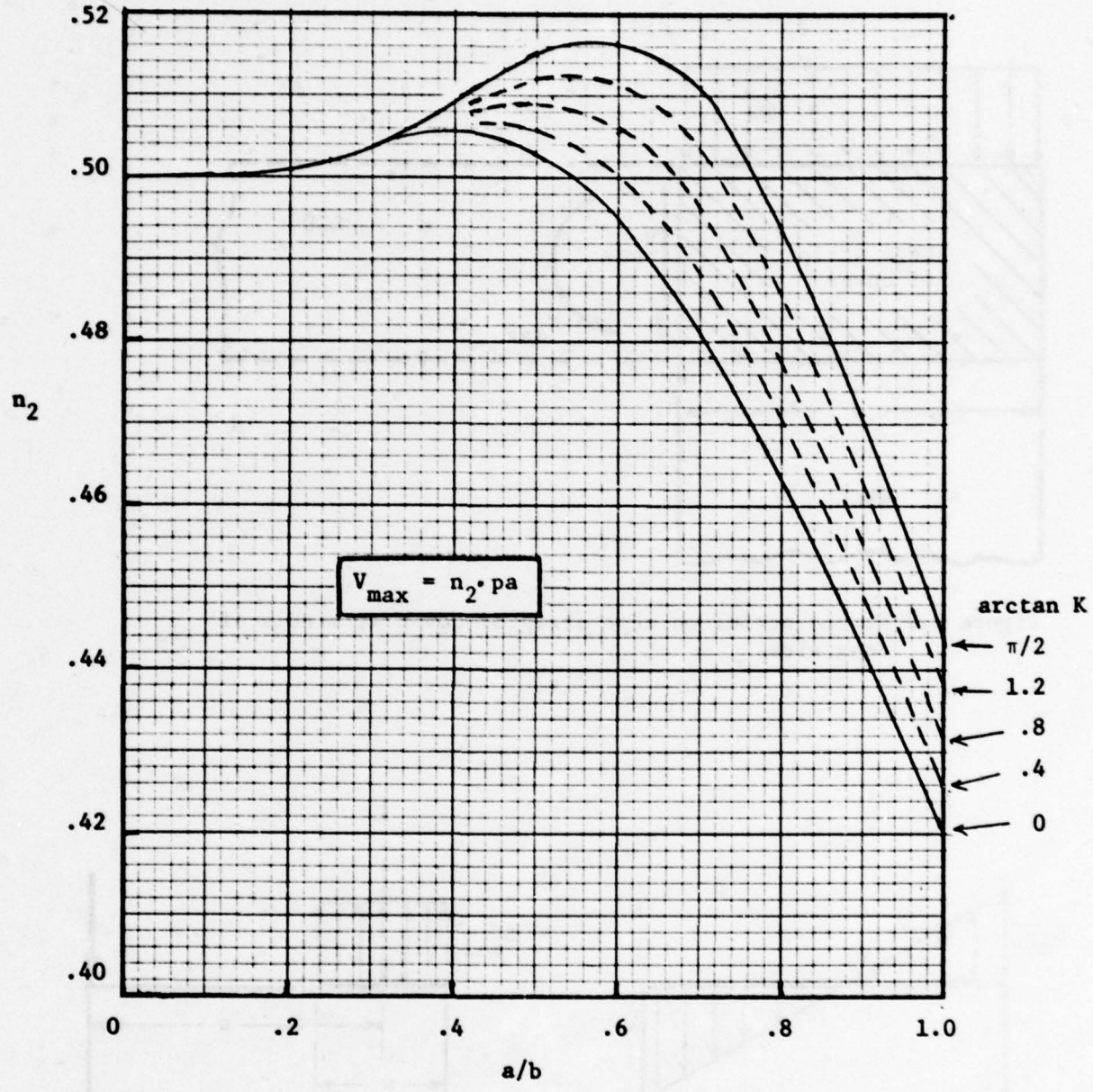

Figure 8.- Intensity of vertical reaction at the middle of the long side for a uniformly loaded rectangular plate obeying Hooke's law with edges elastically restrained against rotation ($\nu = 0.3$)

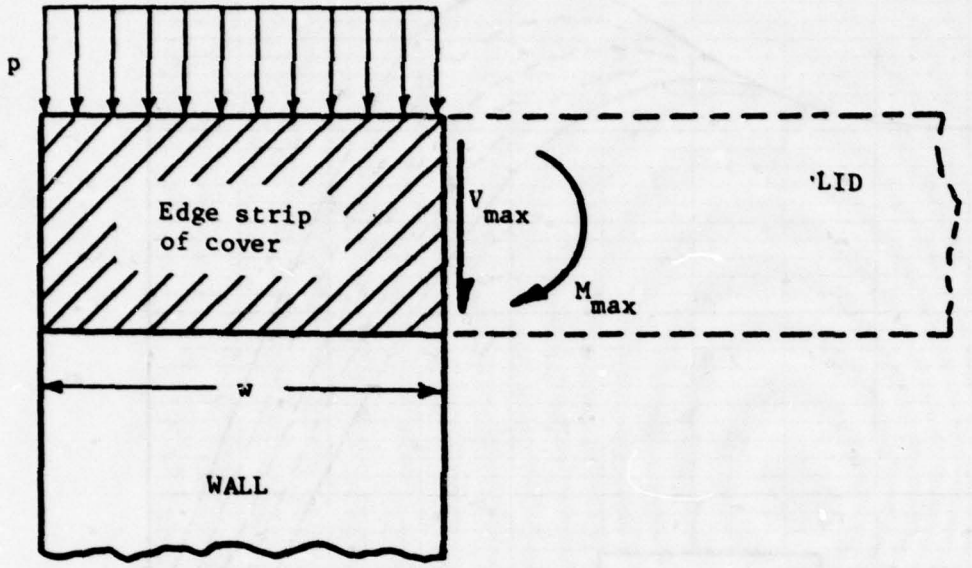

Figure 9.- Forces acting on edge strip of cover at middle of long side.

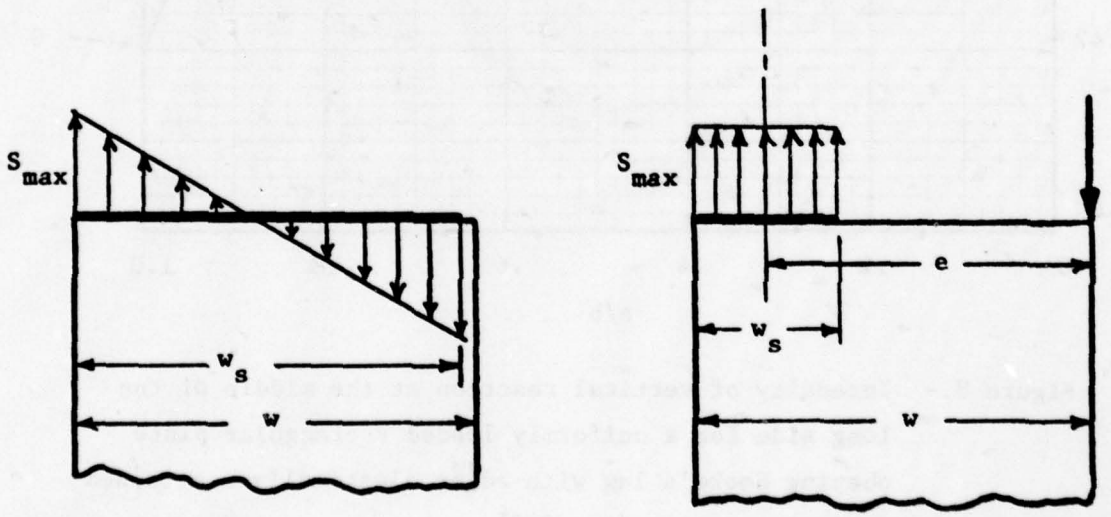

(a) Wide seal ($w_s \approx w$).

(b) Narrow seal ($w_s << w$)

Figure 10.- Stress distributions assumed across top of wall at middle of long side.

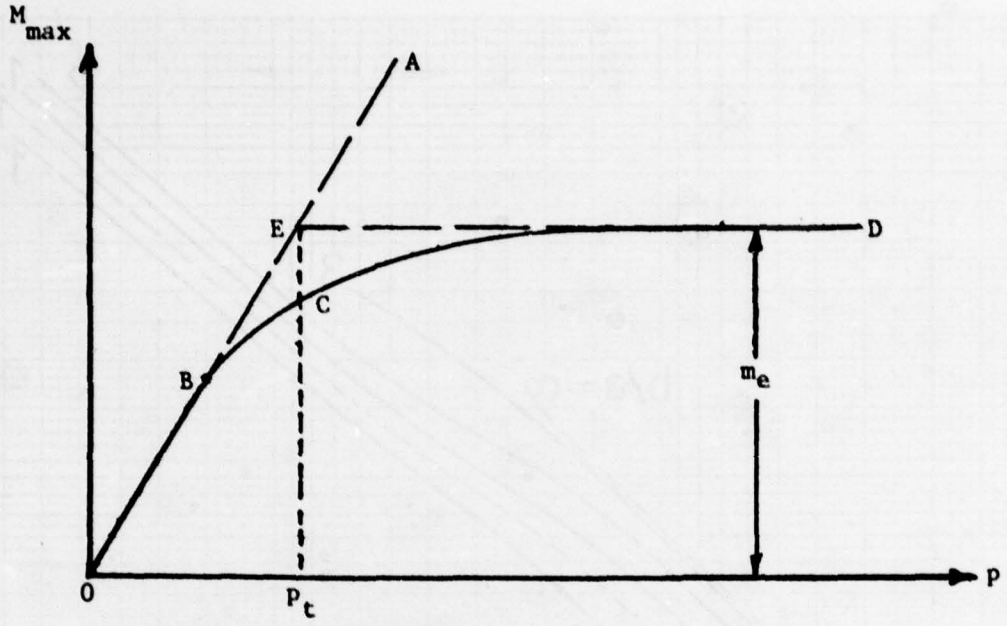

Figure 11.- Relationship between p and M_{max}:

OBEA - Hookean

OBCD - Actual

OBED - Assumed

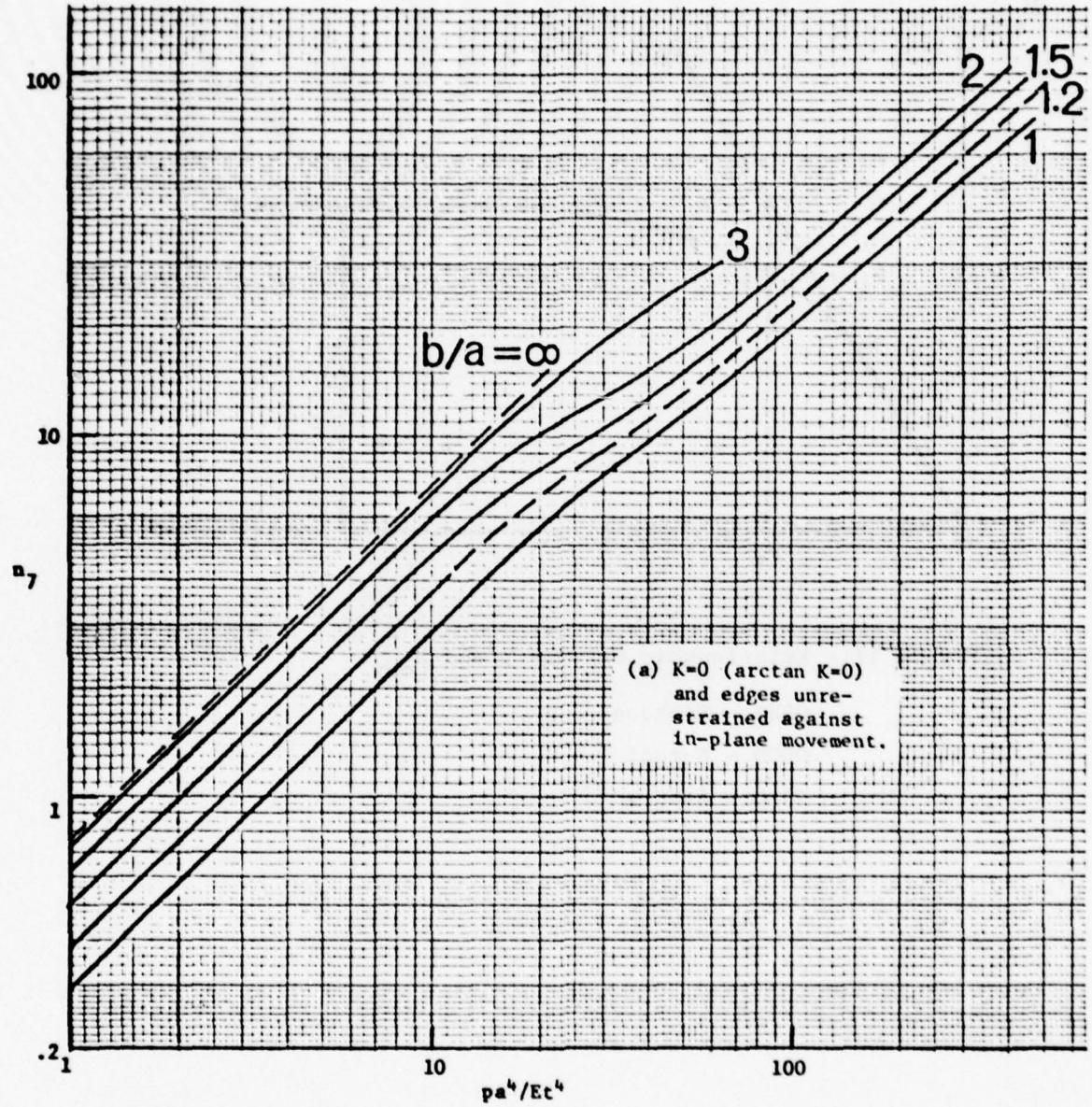

Figure 12.- Graphs for determining the maximum tensile stress σ_{max} in uniformly loaded rectangular plates. Curves adapted from the following parts of Reference 6: (a) top graphs on p. 50, (b) middle graphs on p. 51, (c) middle graphs on p. 50, and (d) middle graphs on p. 52.

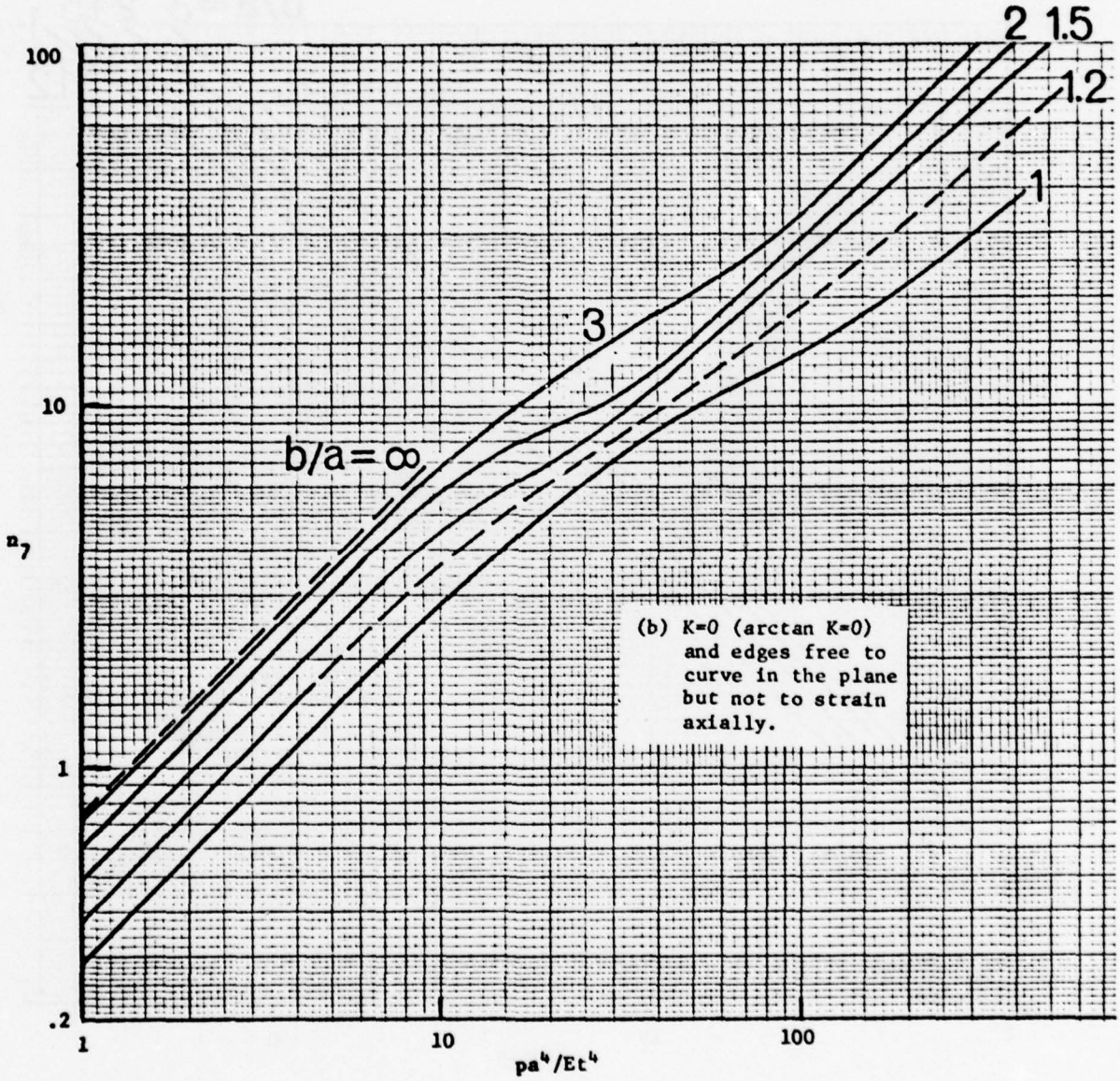

Figure 12.- Continued.

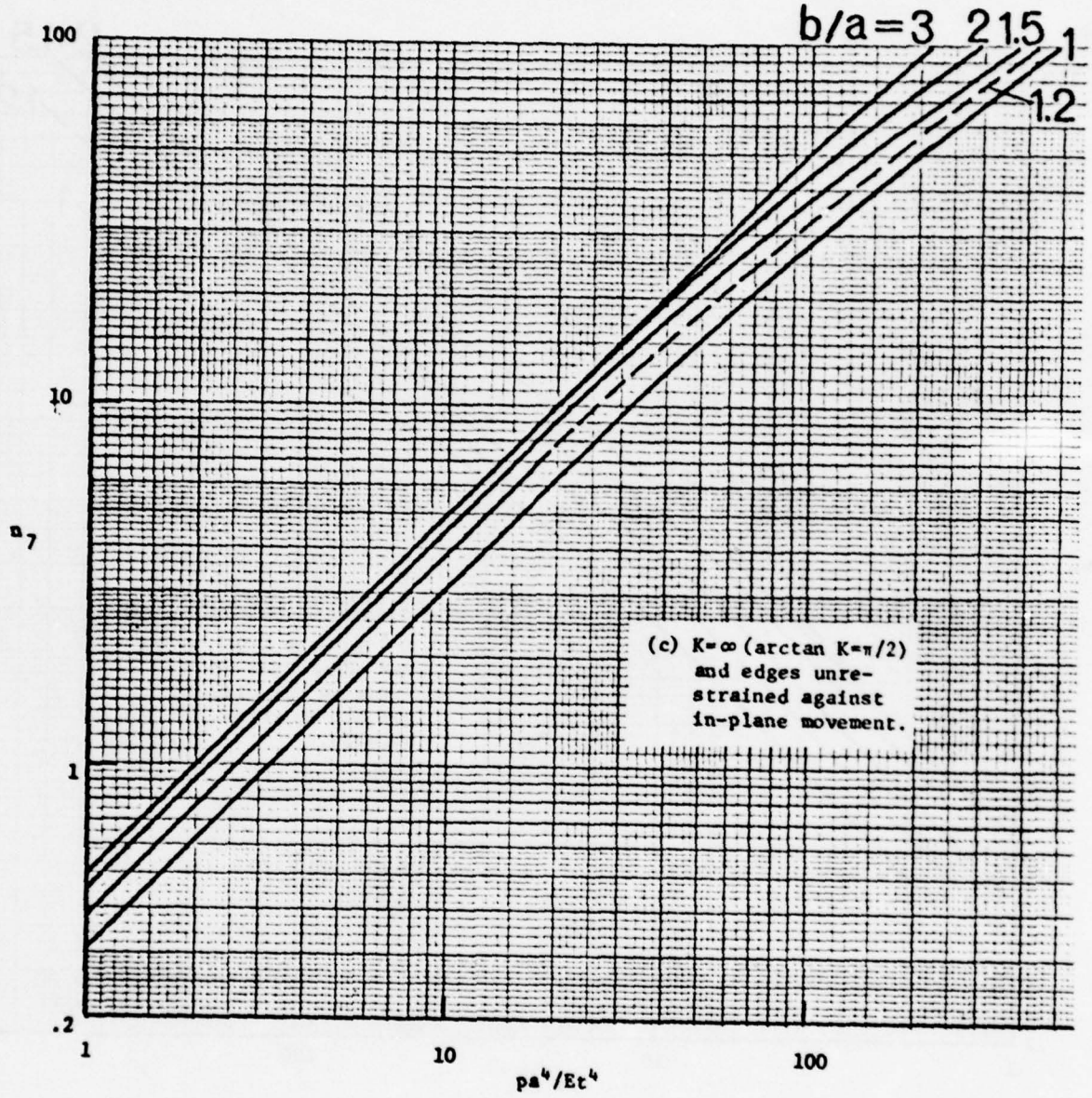

Figure 12.- Continued.

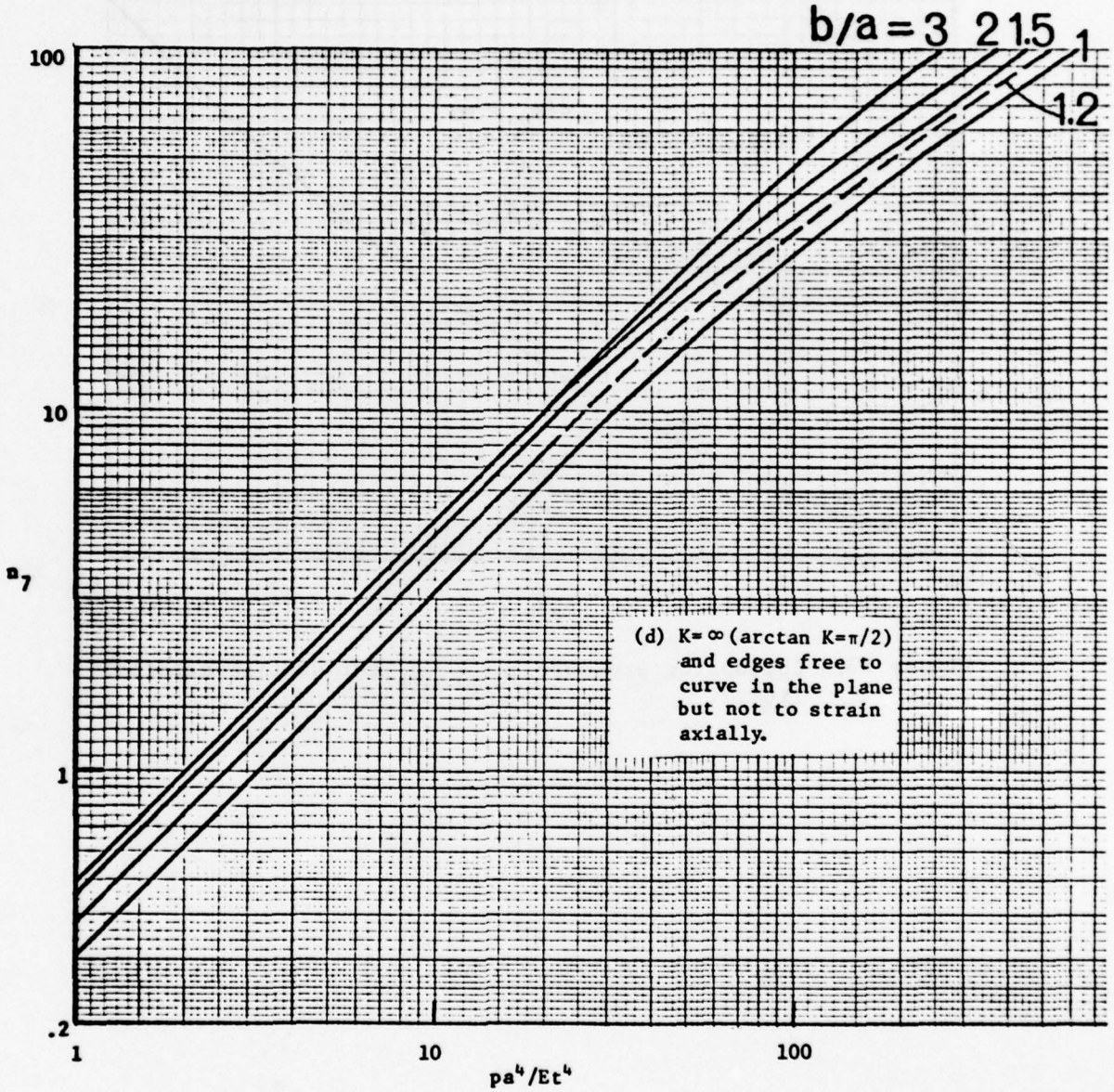

Figure 12.- Concluded.

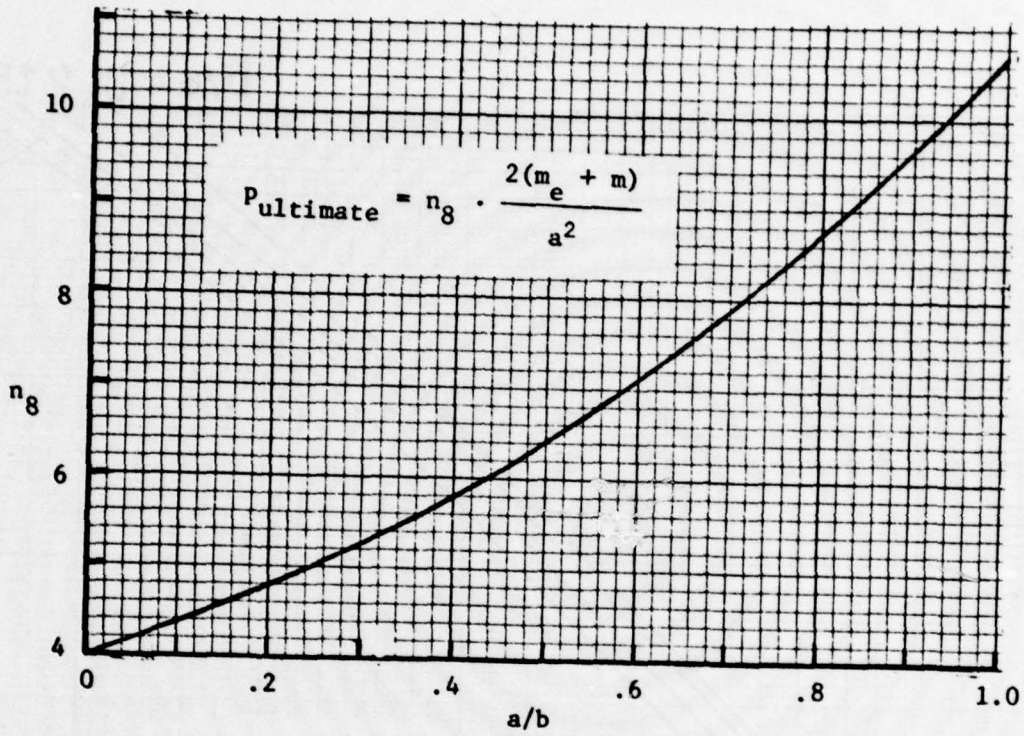

Figure 13.- Collapsing pressure $P_{ultimate}$ for ductile-material lids.

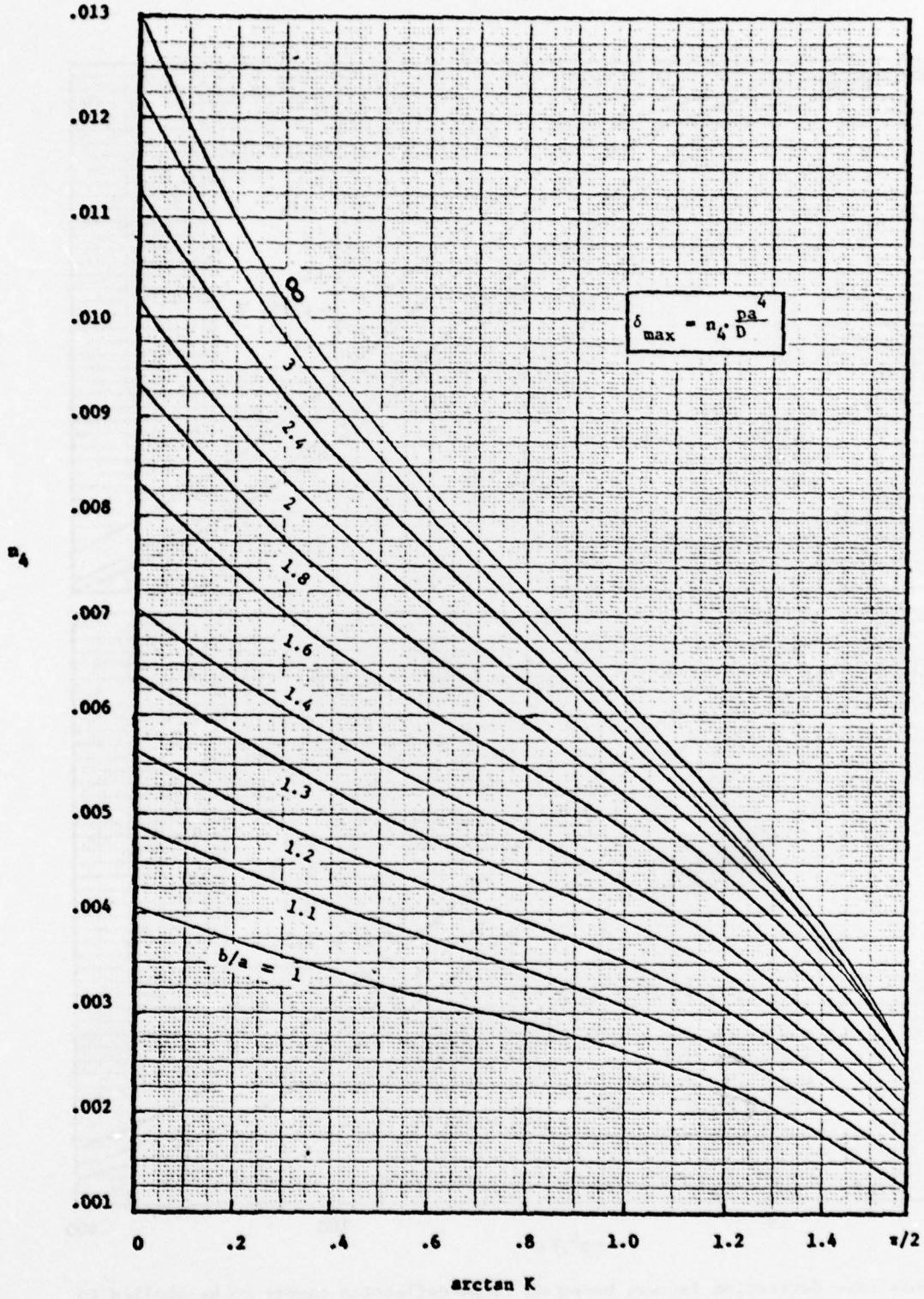

Figure 14.- Center deflection of a uniformly loaded rectangular plate that obeys Hooke's law with edges elastically restrained against rotation (small-deflection theory).

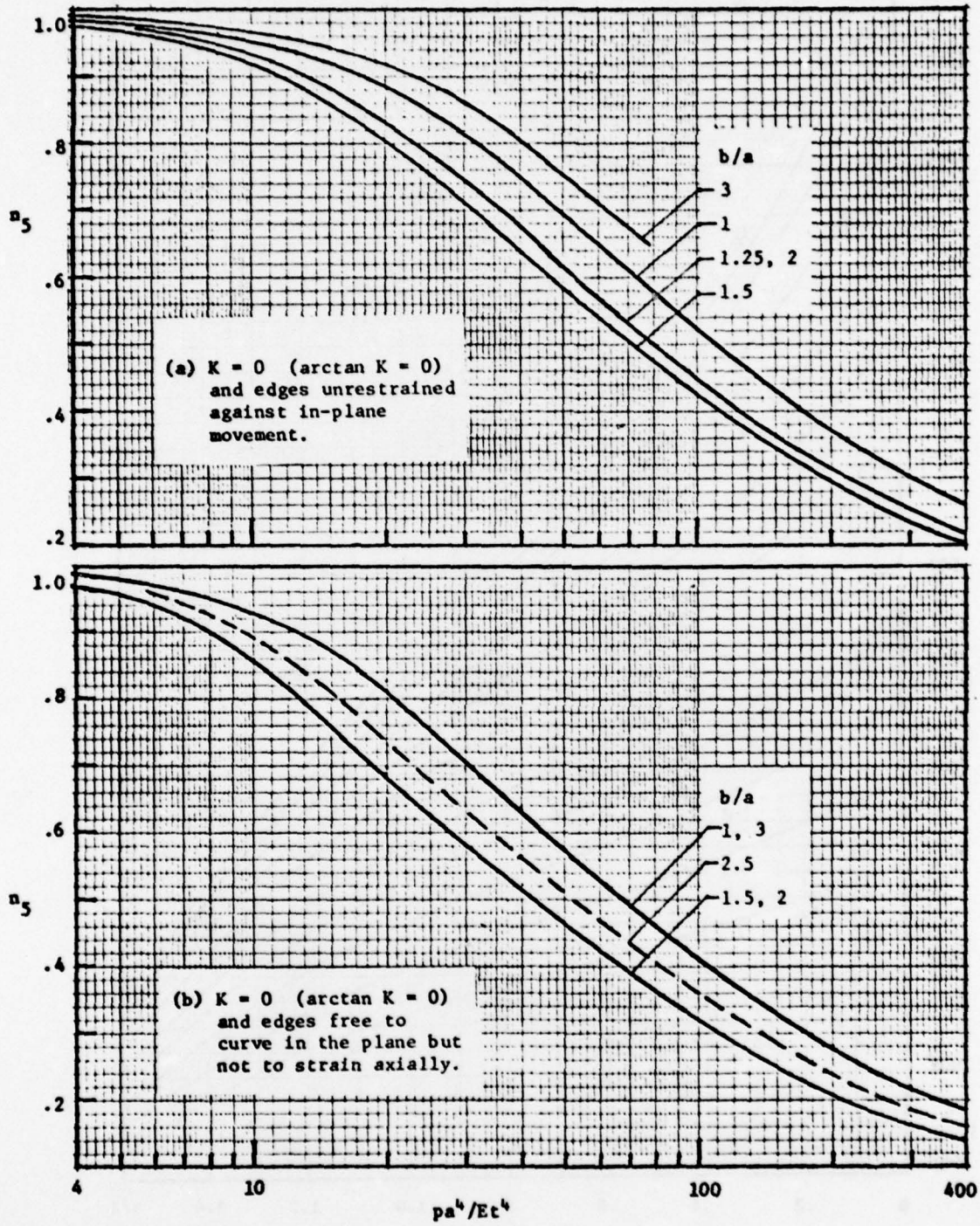

Figure 15.- Correction factors based on large-deflection theory to be applied to small-deflection theory value of center deflection of elastic lid (ν=0.3). Data adapted from: (a) P. 181 of Ref. 5 and p. 150 of Ref. 6. (b) P. 152 of Ref. 6. (c) P. 190 of Ref. 5 and p. 154 of Ref. 6. (c) P. 156 of Ref. 6.

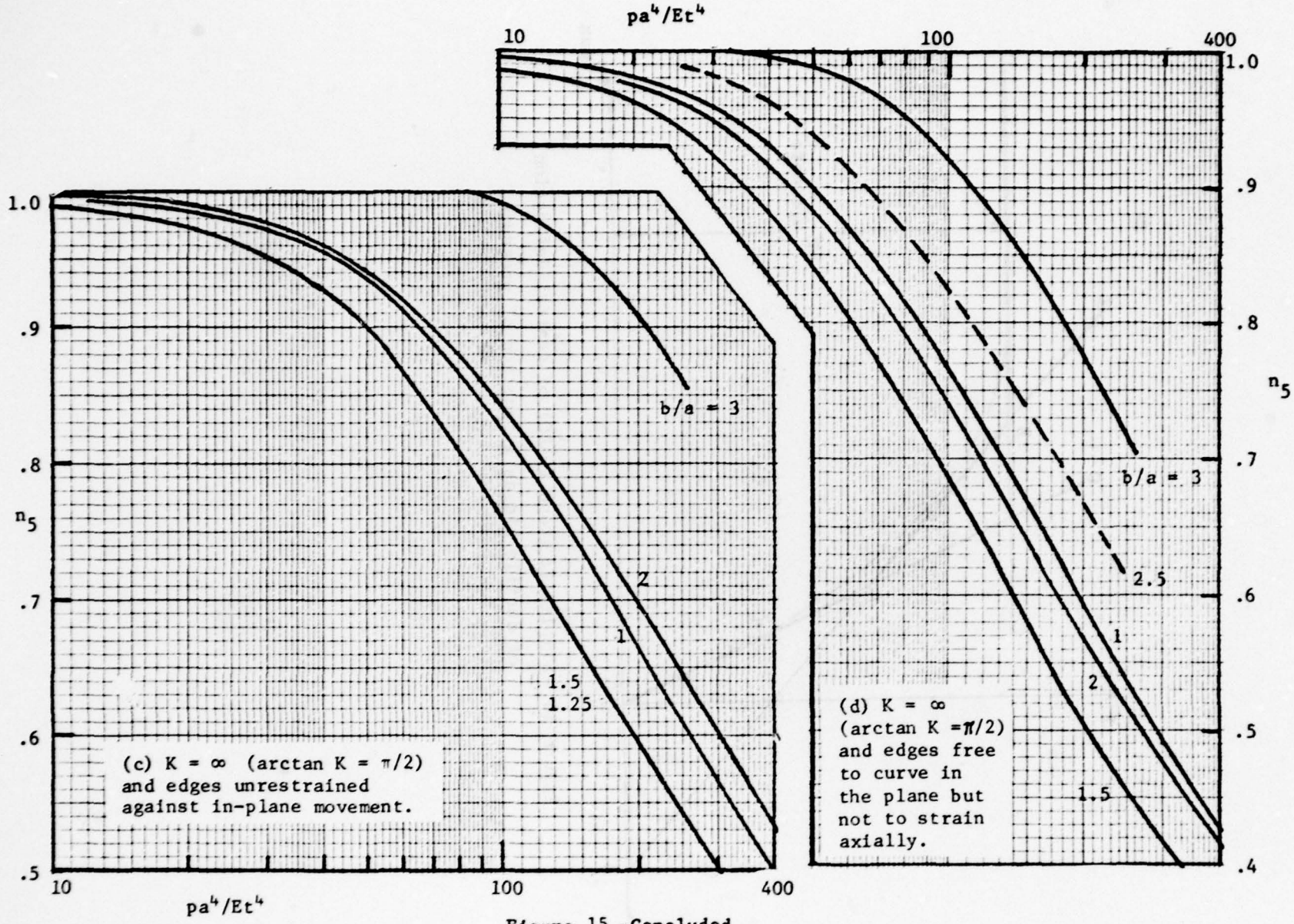

Figure 15.-Concluded.

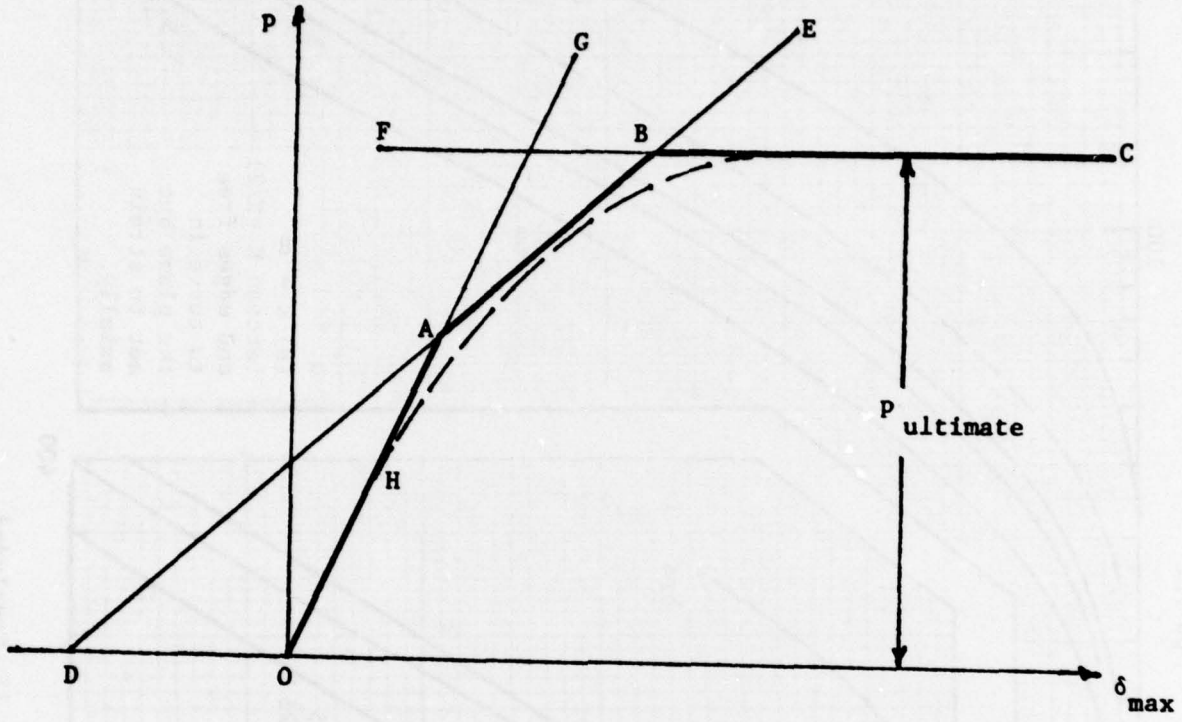

Figure 16.- Simplified graph (OABC) of central deflection of ductile lid as a function of pressure.

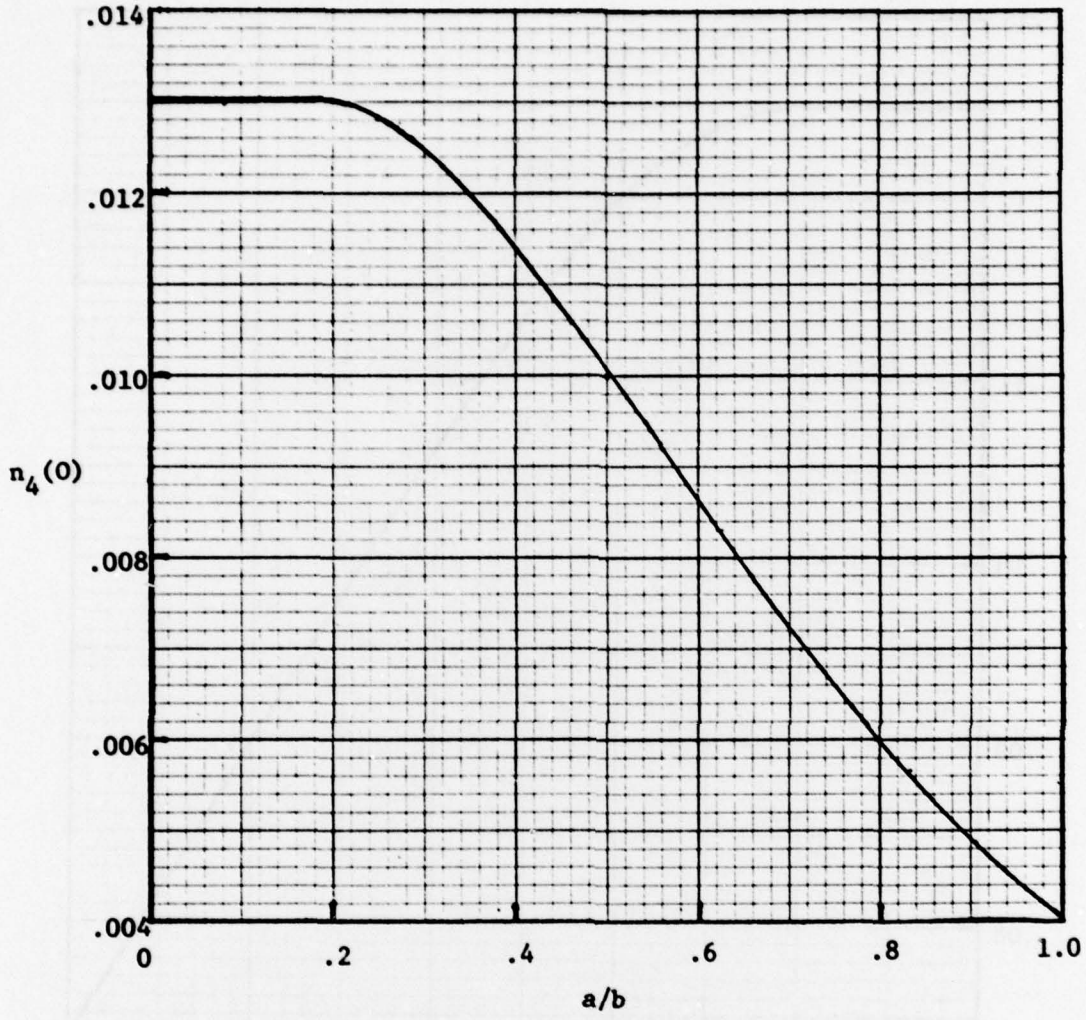

Figure 17.- Graph of $n_4(0)$ as a function of a/b.

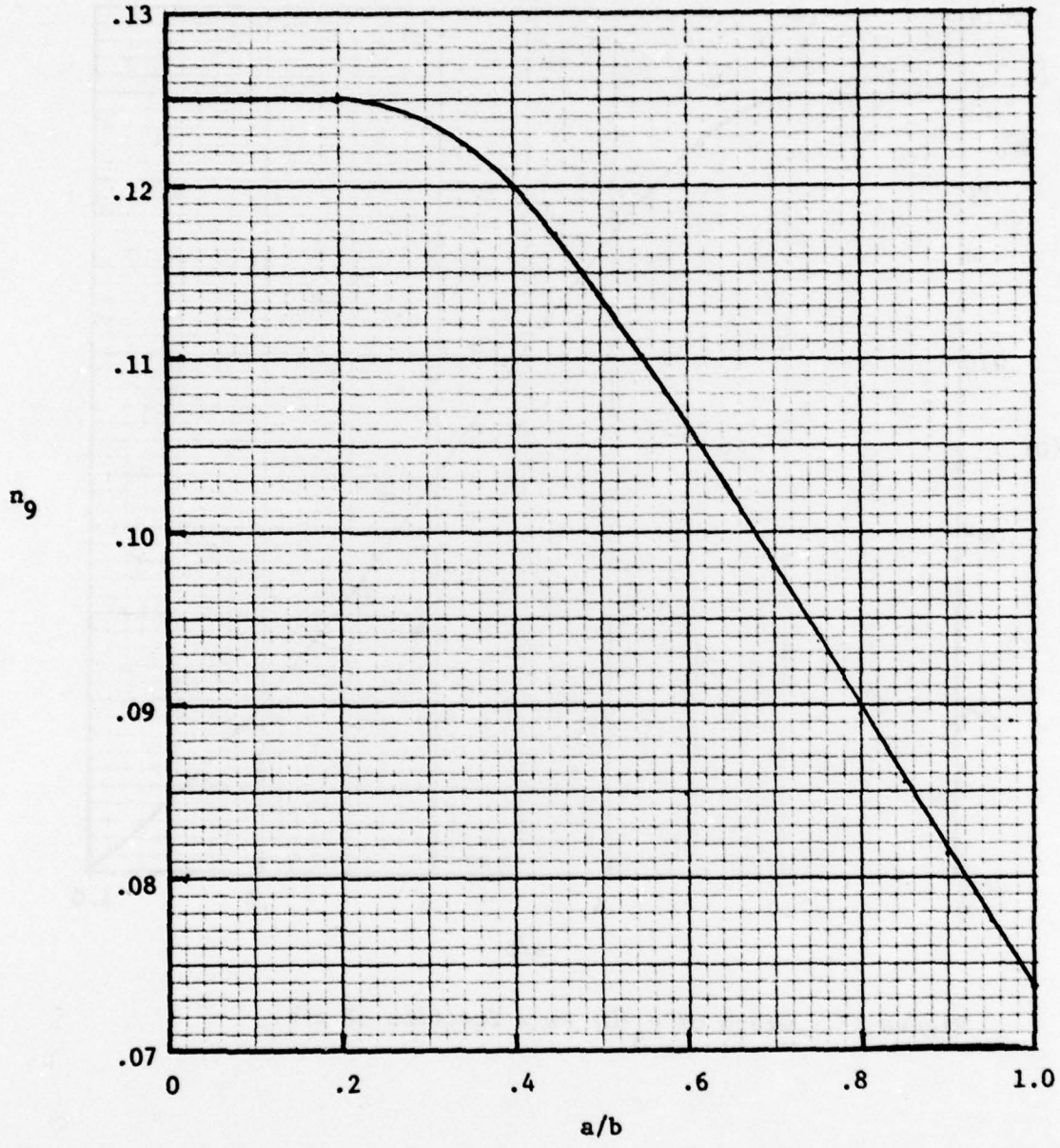

Figure 18.- Graph of n_9 as a function of a/b.

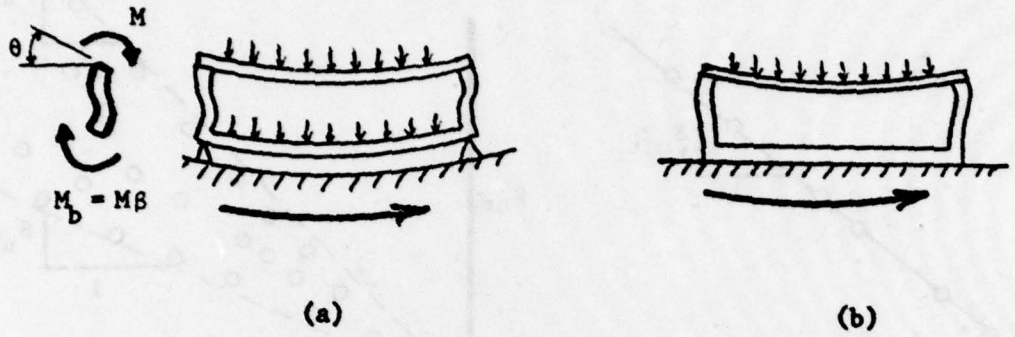

Figure 19.- Two possible kinds of lid-wall-base interaction for a package in a centrifuge.

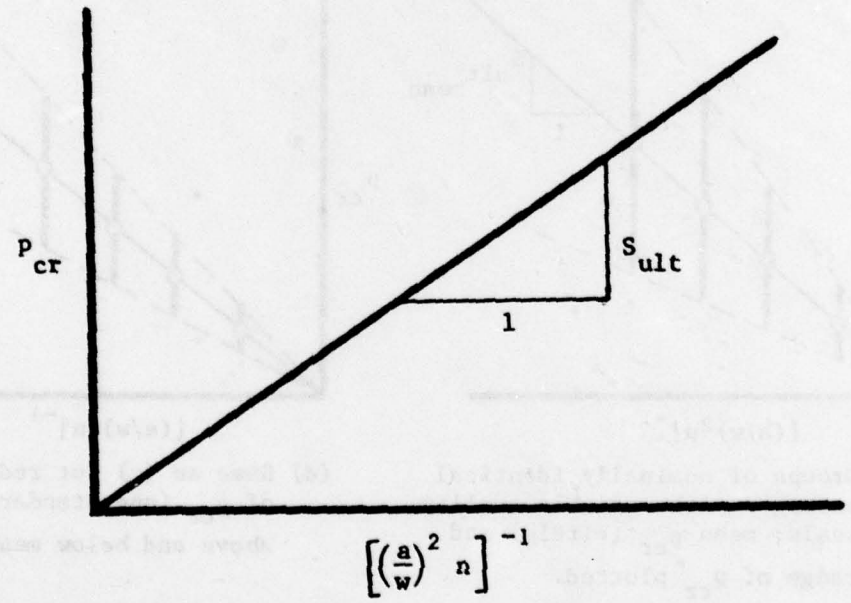

Figure 20.- Relationship implied by Eq. (50) between the pressure p_{cr} causing loss of hermeticity and the package parameter $[(a/w)^2 n]^{-1}$.

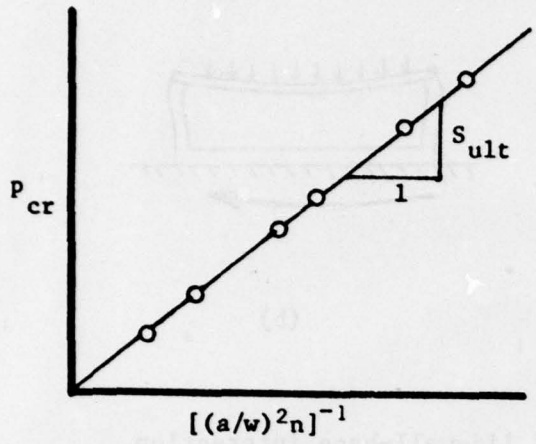

(a) Uniform quality seals.

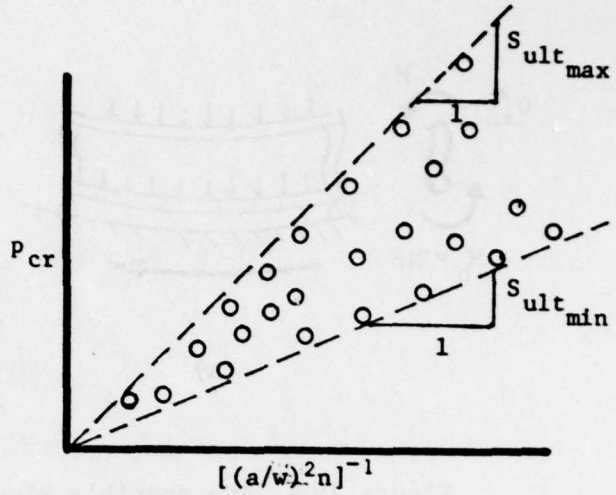

(b) Variable quality seals.

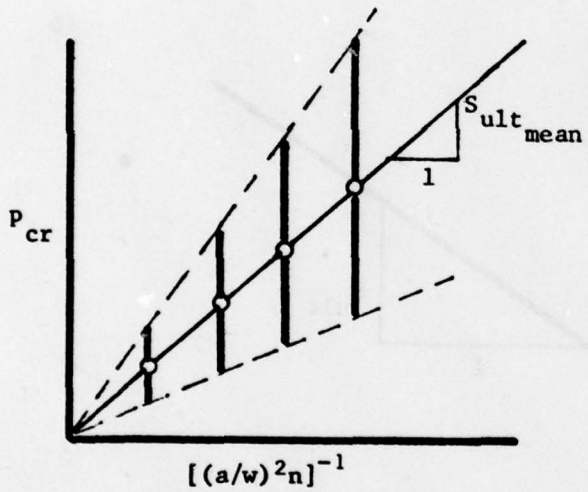

(c) Groups of nominally identical packages with variable quality seals; mean p_{cr} (circle) and range of p_{cr} plotted.

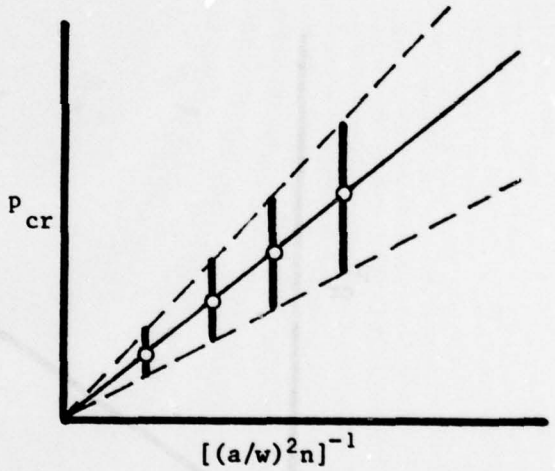

(d) Same as (c) but reduced range of p_{cr} (one standard deviation above and below mean) plotted.

Figure 21.- Hypothetical satisfactory correlations between test data and theory (Eq. (50)).

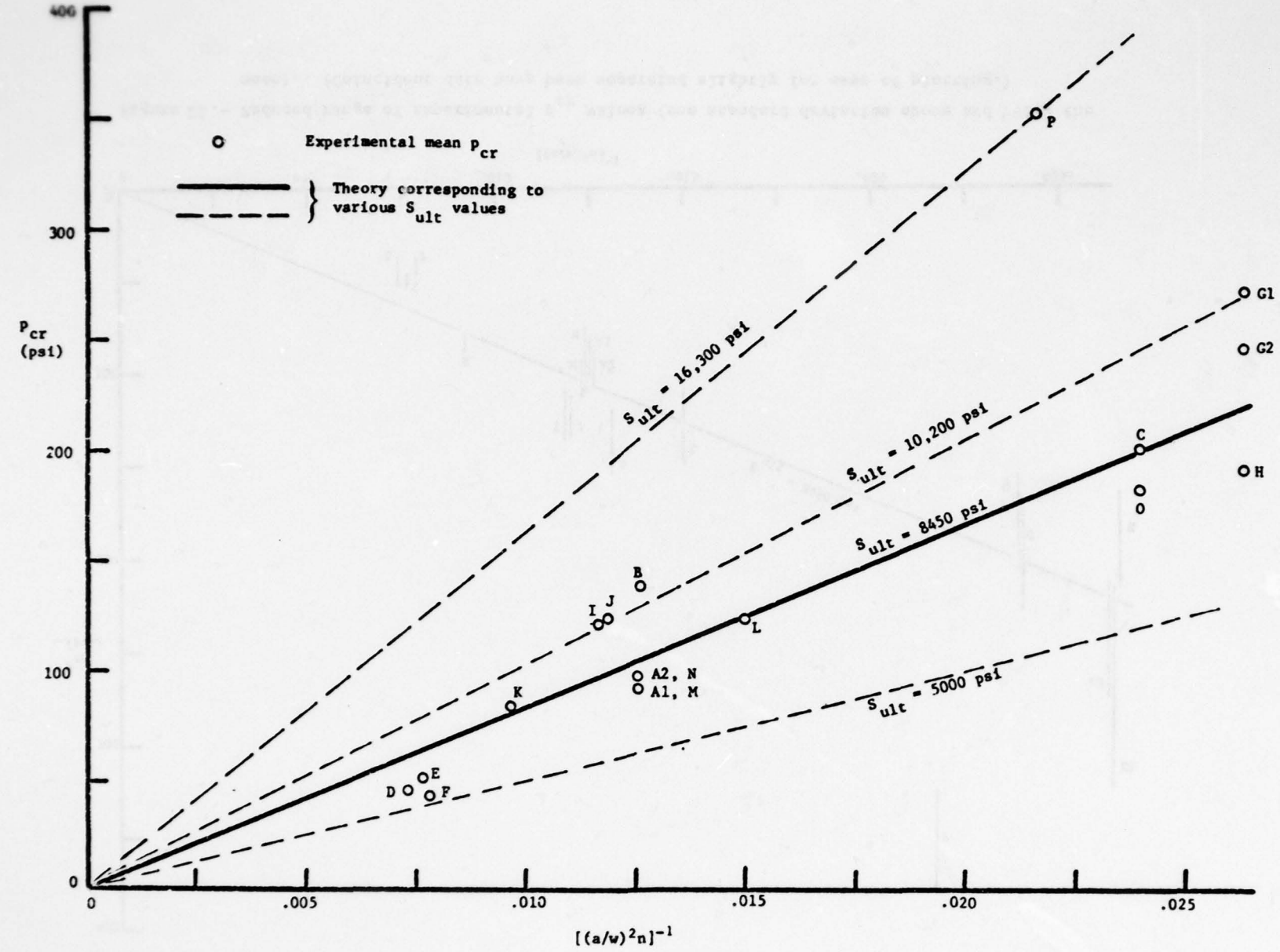

Figure 22.- Mean experimental values of p_{cr} compared with theory.

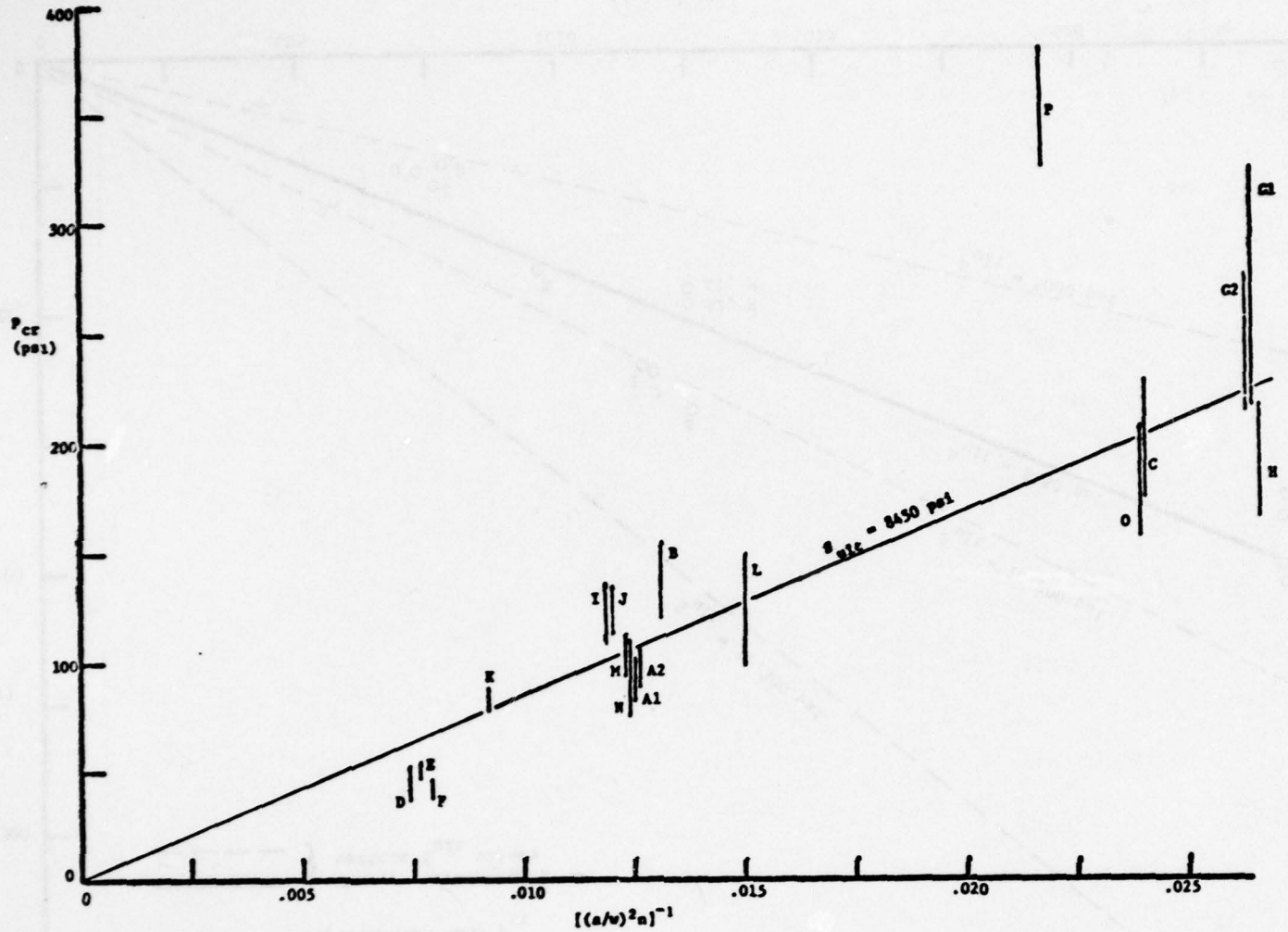

Figure 23.- Reduced range of experimental p_{cr} values (one standard deviation above and below the mean). (Coincident data have been separated slightly for ease of plotting.)

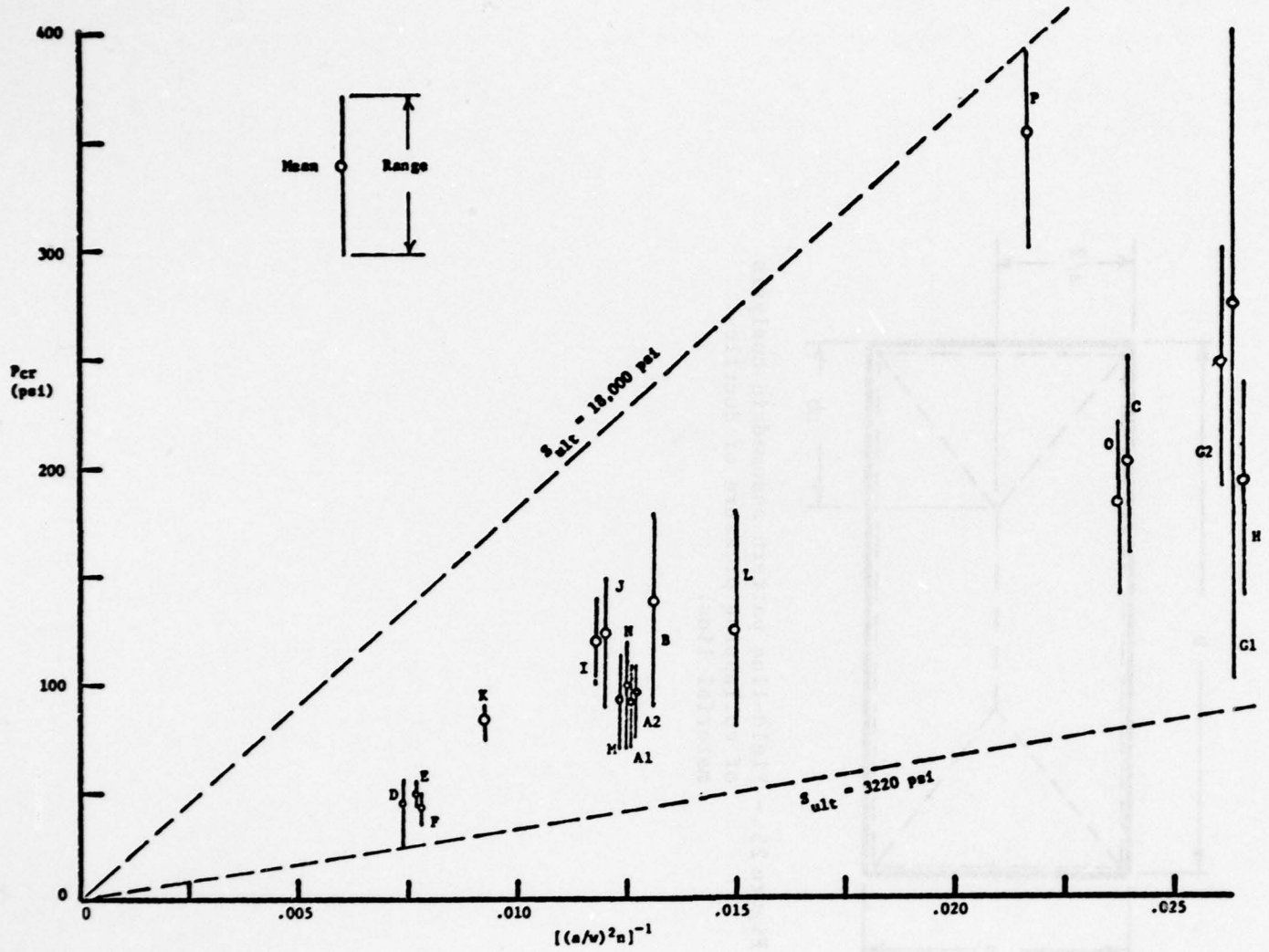

Figure 24.- Full range of experimental p_{cr} values. (Coincident data have been separated slightly for ease of plotting.)

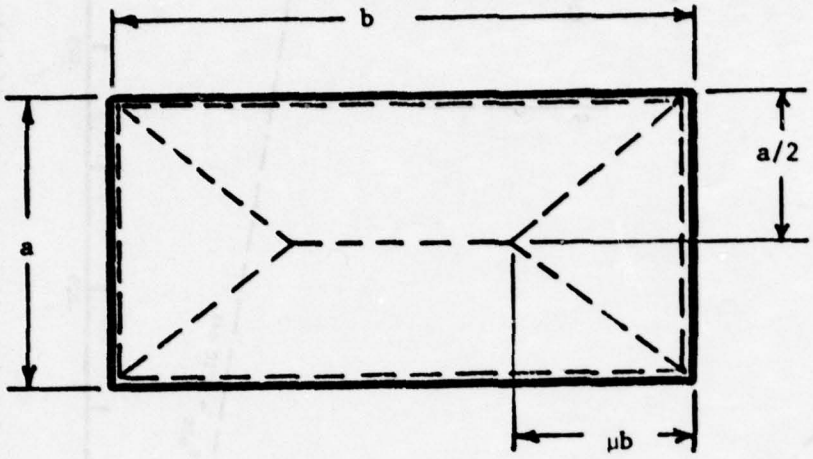

Figure 25 .- Yield-line pattern assumed in analysis of collapsing pressure of ductile-material lids.

MISSION
of
Rome Air Development Center

RADC plans and executes research, development, test and selected acquisition programs in support of Command, Control Communications and Intelligence (C^3I) activities. Technical and engineering support within areas of technical competence is provided to ESD Program Offices (POs) and other ESD elements. The principal technical mission areas are communications, electromagnetic guidance and control, surveillance of ground and aerospace objects, intelligence data collection and handling, information system technology, ionospheric propagation, solid state sciences, microwave physics and electronic reliability, maintainability and compatibility.